The Frontiers of Observational Cosmology and the Confrontation with Theory

Malcolm Longair,

Cavendish Laboratory, Cambridge

Programme

- Basic observations on which the models are based.
- Testing the basic assumptions made in the construction of the standard cosmological models.
- Structure formation in the standard models
- Observational tests of the standard models – the confrontation with observation
- Basic problems and approaches to their solution
- Future observational challenges – EUCLID as an example.

For illustrative purposes: $\Omega_0 = 0.3$, $\Omega_\Lambda = 0.7$, $h = 0.7$.

COBE Observations of the Cosmic Microwave Background Radiation

T = 2.728 K

ΔT = 3.353 mK

ΔT = 18 μK

Whole sky in Hammer-Aitoff projection
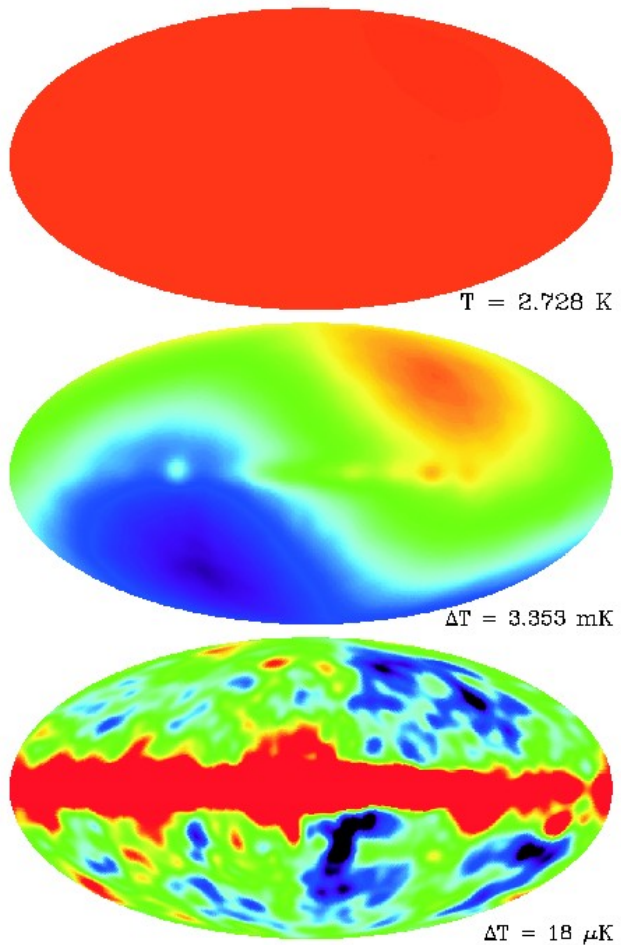
- The spectrum very precisely that of a perfect black-body at T = 2.726 K.

- A perfect dipole component is detected, corresponding to the motion of the Earth through the frame in which the radiation would be perfectly isotropic.

- Away from the Galactic plane, isotropy to better than one part in 10^5. Significant temperature fluctuations $\Delta T/T \approx 10^{-5}$ detected on scales $\theta \geq 7°$
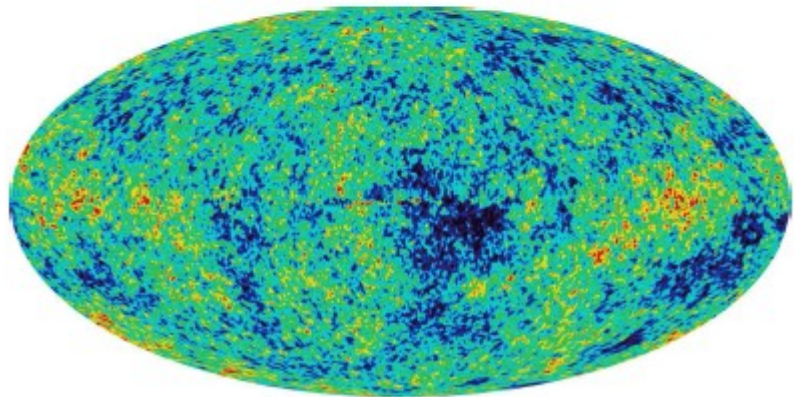
WMAP Observations of the Cosmic Microwave Background Radiation (2003)
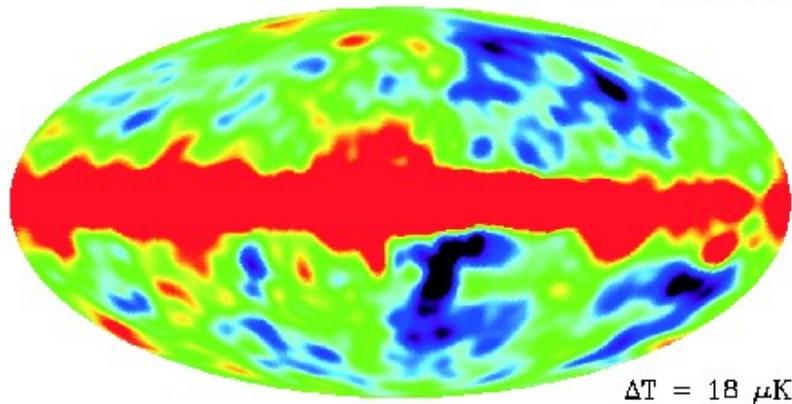
Cosmic Background Explorer (COBE): $\theta = 7°$.

The same features present in the WMAP image of the sky. The WMAP experiment had much higher angular resolution than COBE.
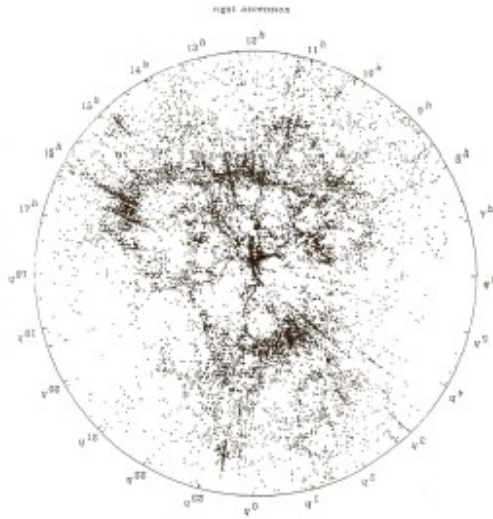
Wilkinson Microwave Anisotropy Probe (WMAP) $\theta = 0.3°$.

Galactic foreground emission has been subtracted.

The radiation originated on the last scattering surface at a redshift $z \sim 1000$, or scale factor $a \sim 10^{-3}$.

The Homogeneity of the Universe

The homogeneity of the Universe has been established by large surveys of galaxies, starting with the local distribution determined by Geller and Huchra.
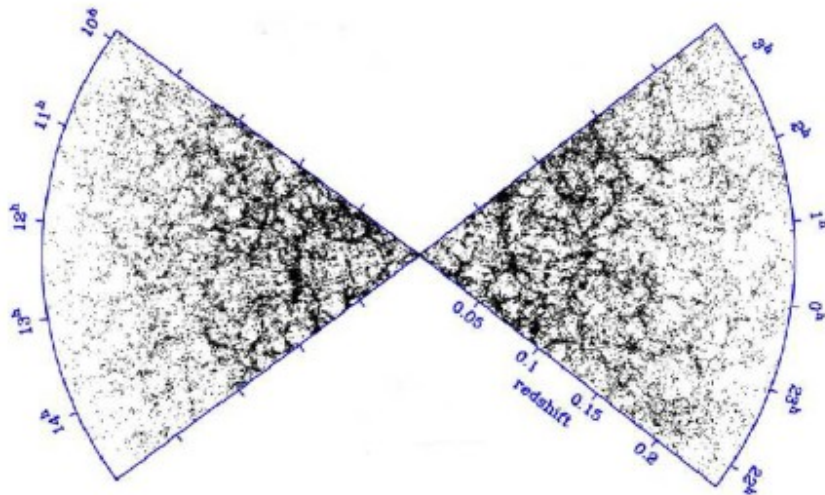
On the largest scales accessible at the present epoch the 2dF and SDSS surveys, each containing over 200,000 galaxies, show the same cellular structure

The Homogeneity of the Universe
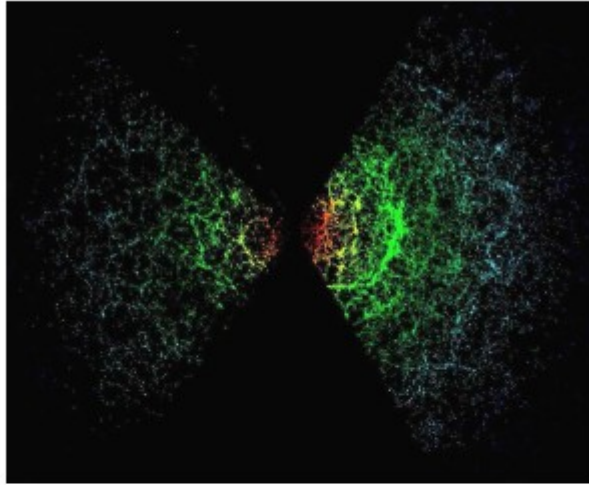
The Sloan Digital Sky Survey shows the same irregular large scale distribution of galaxies with giant walls and holes on scales much greater than those of clusters of galaxies.

The galaxy distribution displays the same degree of inhomogeneity as we observe to larger distances in the Universe as demonstrated by the scaling of the two-point correlation functions for galaxies
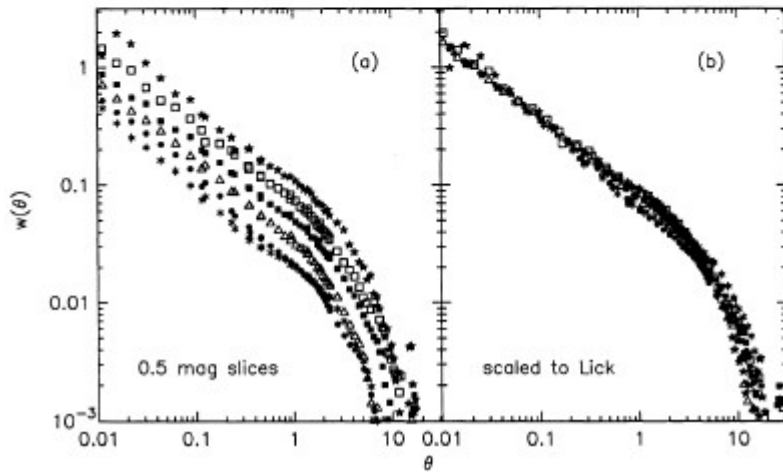
$$n(r) = n_0[1+\xi(r)]$$

Notice: We are no longer observing the distant Universe through a non-distorting screen.
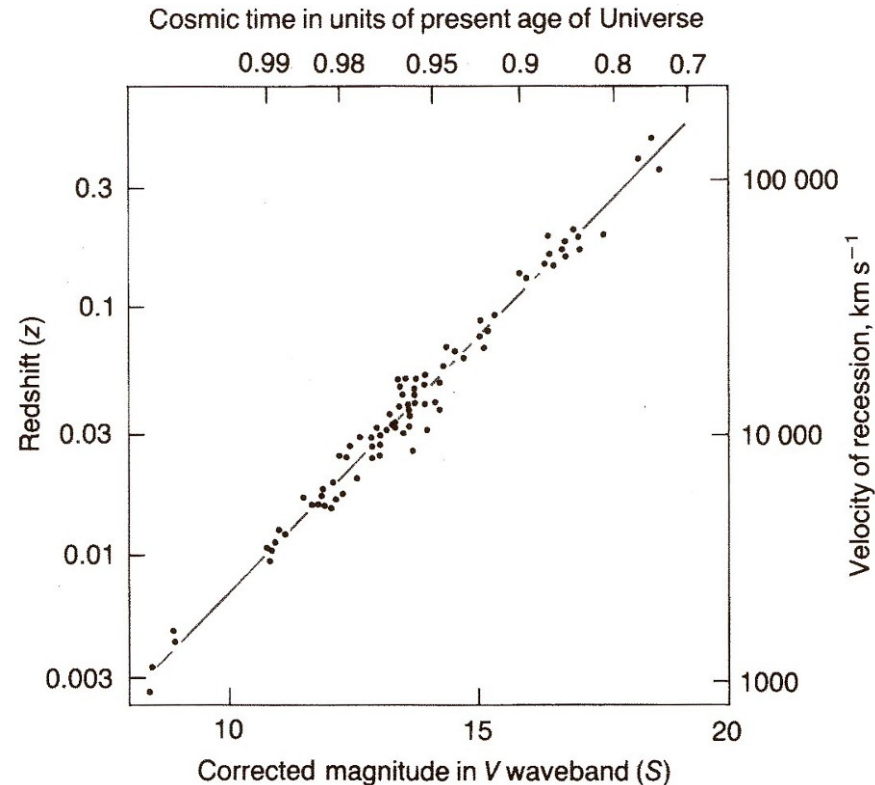
Hubble's Law

The second result we need is the redshift-distance relation for galaxies – the Hubble diagram. A modern version of Hubble's law for the brightest galaxies in rich clusters of galaxies is shown ,

$$v = H_0 r.$$

H_0 is Hubble's constant. All classes of galaxy follow the same Hubble's law.

This means that the Universe as a whole is expanding uniformly.

Basic Assumptions

The standard models are based upon two assumptions and a theory of gravity:

- The *Cosmological Principle* – we are not located at any special location in the Universe. Combined with the observations that the Universe is isotropic, homogeneous and uniformly expanding on a large scale, this leads to the Robertson–Walker metric.

- *Weyl's Postulate* is the statement that the world lines of particles meet at a singular point in the finite or infinite past. This solves the clock synchronisation problem and means that there is a unique world line passing through every point in space-time. The fluid behaves like a perfect fluid with energy–momentum tensor $T^{\alpha\beta}$.

- *General Relativity,* which enables us to relate the energy–momentum tensor to the geometrical properties of space-time.

The Robertson-Walker Metric

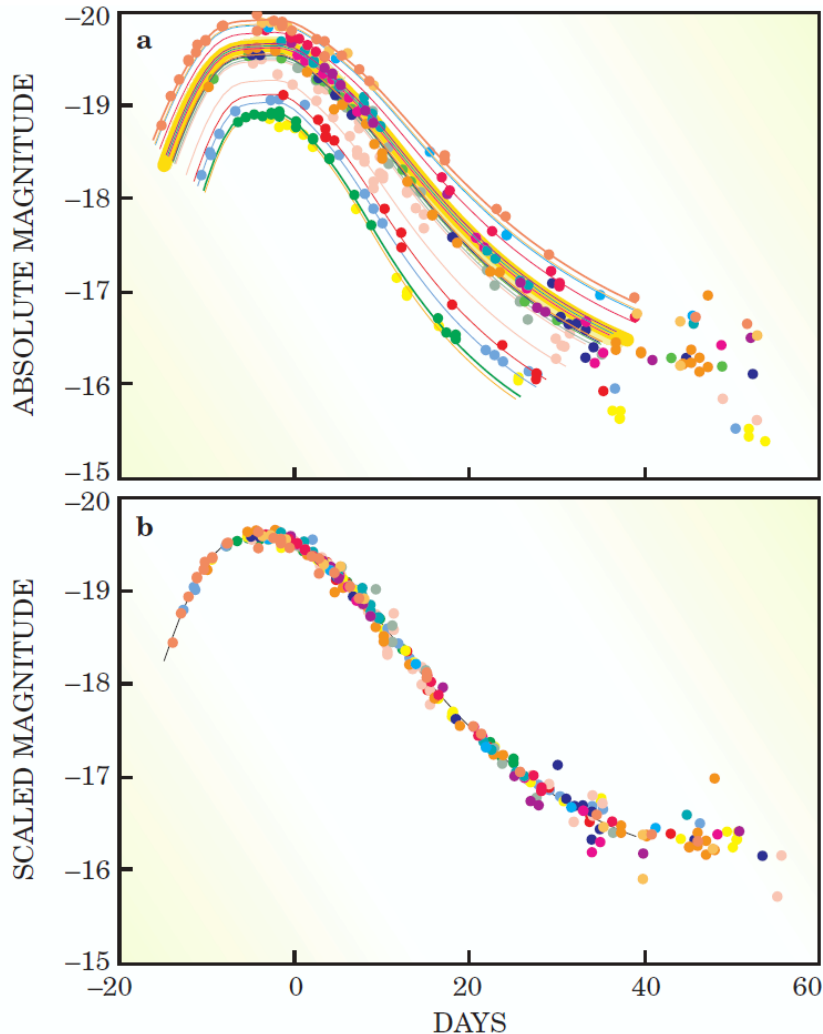The *Robertson-Walker metric* can be written in the following form:

$$\mathrm{d}s^2 = \mathrm{d}t^2 - \frac{a^2(t)}{c^2}[\mathrm{d}r^2 + \mathfrak{R}^2 \sin^2(r/\mathfrak{R})(\mathrm{d}\theta^2 + \sin^2\theta\,\mathrm{d}\phi^2)] \, .$$

t is cosmic time as measured by a clock carried by a fundamental observer and r is the *comoving radial distance coordinate* which is fixed to a galaxy for all time.

The metric contains one unknown function $a(t)$, the scale factor, and the constant $\mathfrak{R}$, the radius of curvature of the geometry of the Universe at the present epoch. It follows from the R-W metric that the redshift $z = (\lambda_0 - \lambda_e)/\lambda_e$ is directly related to the scale-factor through the relation

$$a(t) = \frac{1}{1+z}.$$

The Time Dilation Test

A key test of the Robertson-Walker metric is that the same formula which describes the redshift of spectral lines should also apply to time intervals in the emitted and received reference frames.

Type 1a supernova have remarkably similar light curves (top). The relation becomes even tighter when account is taken of the luminosity-width correlation (bottom)

The Time Dilation Test
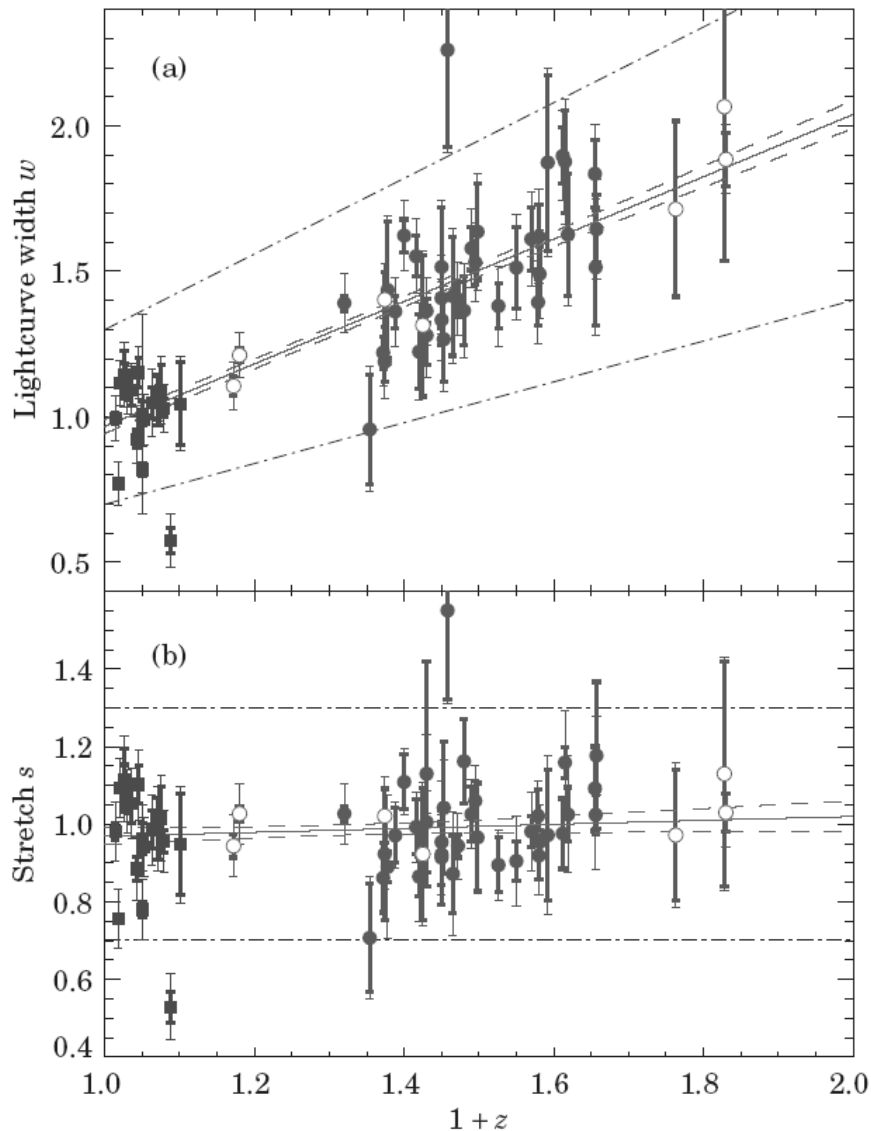
A clear time dilation effect is observed exactly proportional to (1+z), as predicted by the Robertson-Walker metric. These data include corrections for the luminosity-width relation.

The width of the light curves divided by (1+z).

The Radiation Temperature Test

In the case of black-body radiation, the energy density of the radiation is given by the Stefan–Boltzmann law $\varepsilon = aT^4$ and its spectral energy density by the Planck distribution

$$\varepsilon(\nu)\,\mathrm{d}\nu = \frac{8\pi h \nu^3}{c^3}\frac{1}{e^{h\nu/kT}-1}\,\mathrm{d}\nu\ .$$

It immediately follows that, for black-body radiation, the radiation temperature T_r varies with redshift as $T_r = T_0(1+z)$ and the spectrum of the radiation changes as

$$
\begin{aligned}
\varepsilon(\nu_1)\,\mathrm{d}\nu_1 &= \frac{8\pi h \nu_1^3}{c^3}[(e^{h\nu_1/kT_1}-1)]^{-1}\,\mathrm{d}\nu_1 \\
&= \frac{8\pi h \nu_0^3}{c^3}[e^{h\nu_0/kT_0}-1)^{-1}](1+z)^4\,\mathrm{d}\nu_0 \\
&= (1+z)^4\,\varepsilon(\nu_0)\,\mathrm{d}\nu_0\ .
\end{aligned}
$$

The Radiation Temperature Test

The temperature of the background radiation can be inferred from observations of fine structure lines in the spectra of distant quasars. The photons of the background radiation excite the fine-structure levels of the ground state of the neutral carbon (CI) atoms and the relative strengths of the absorption lines originating from the ground and first excited states are determined by the temperature of the background radiation.

| Author	quasar	redshift	predicted	observed
Songaila et al. (1994)	Q1331+170	$z_{abs} = 1.776$	7.58 K	7.4 ± 0.8
Ge et al. (1997)	QSO 0013-004	$z_{abs} = 1.9731$	8.105 K	7.9 ± 1.0 K
Ledoux et al. (2006)	PSS J1443+2724	$z_{abs} = 4.224$	14.2 K	consistency

Testing General Relativity
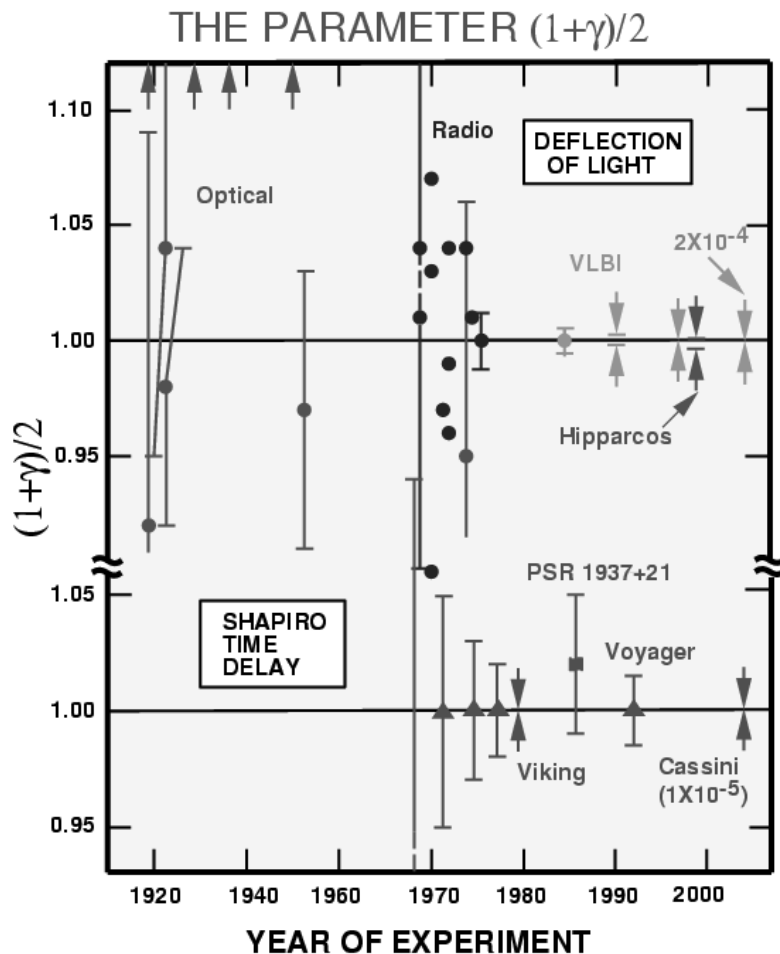
Measurements of the quantity $(1+\gamma)/2$ from light deflection and time delay experiments. The value of γ according to General Relativity is unity. The time-delay measurements from the Cassini spacecraft yielded agreement with General Relativity at the level of 10^{-3} percent. VLBI radio deflection measurements have reached 0.02 percent accuracy. The *Hipparcos limits* were derived from precise measurements of the positions stars over the whole sky and resulted in a precision of 0.1 percent in the measurement of γ.

The Four Tests of General Relativity

- *Gravitational Redshift of electromagnetic waves in a gravitational field.* Hydrogen masers in rocket payloads confirm the prediction at the level of about 5 parts in 10^5.

- The *Advance of the Perihelion of Mercury.* Continued observations of Mercury by radar ranging have established the advance of the perihelion of its orbit to about 0.1% precision with the result $d\omega/dt = 42.98(1 \pm 0.001)$ arcsec per century. General Relativity predicts a value of $d\omega/dt = 42.98$ arcsec per century.

- *Gravitational Deflection of Light by the Sun* has been measured by VLBI and the values found are $(1+\gamma)/2 = 0.99992 \pm 0.00023$.

- *Time Delay of Electromagnetic Waves* propagating through a varying gravitational potential. The Cassini spacecraft found a time-delay corresponding to $(\gamma - 1) = (2.1 \pm 2.3) \times 10^{-5}$. Hence the coefficient $(1+\gamma)/2$ must be within at most 0.0012 percent of unity.

Testing General Relativity – Binary Pulsars

Magnetic axis

Rotation axis

Gravitational waves

Pulsar PSR 1913+16

A schematic diagram of the orbit of the binary pulsar PSR 1913+16. The pulsar is one of a pair of neutron stars in binary orbits about their common centre of mass. There is displacement between the axis of the magnetic dipole and the rotation axis of the neutron star. The radio pulses are assumed to be due to beams of radio emission from the poles of the magnetic field distribution. Many parameters of the binary orbit and the masses of the neutron stars can be measured with very high precision by accurate timing measurements.
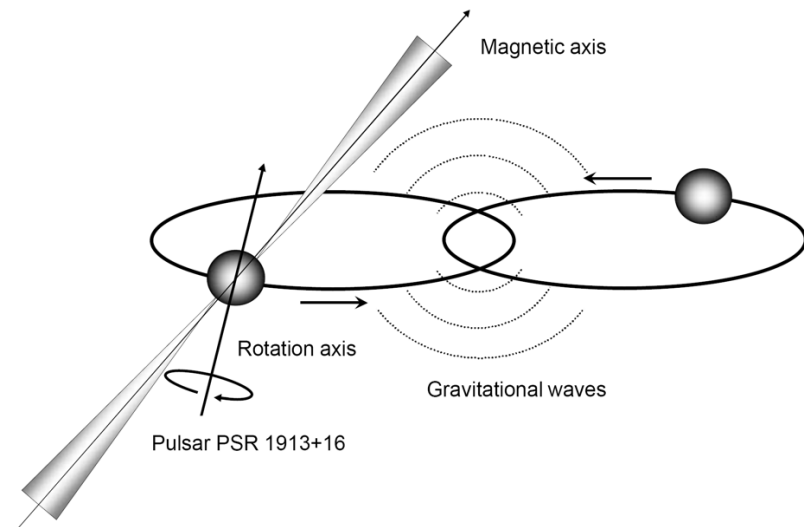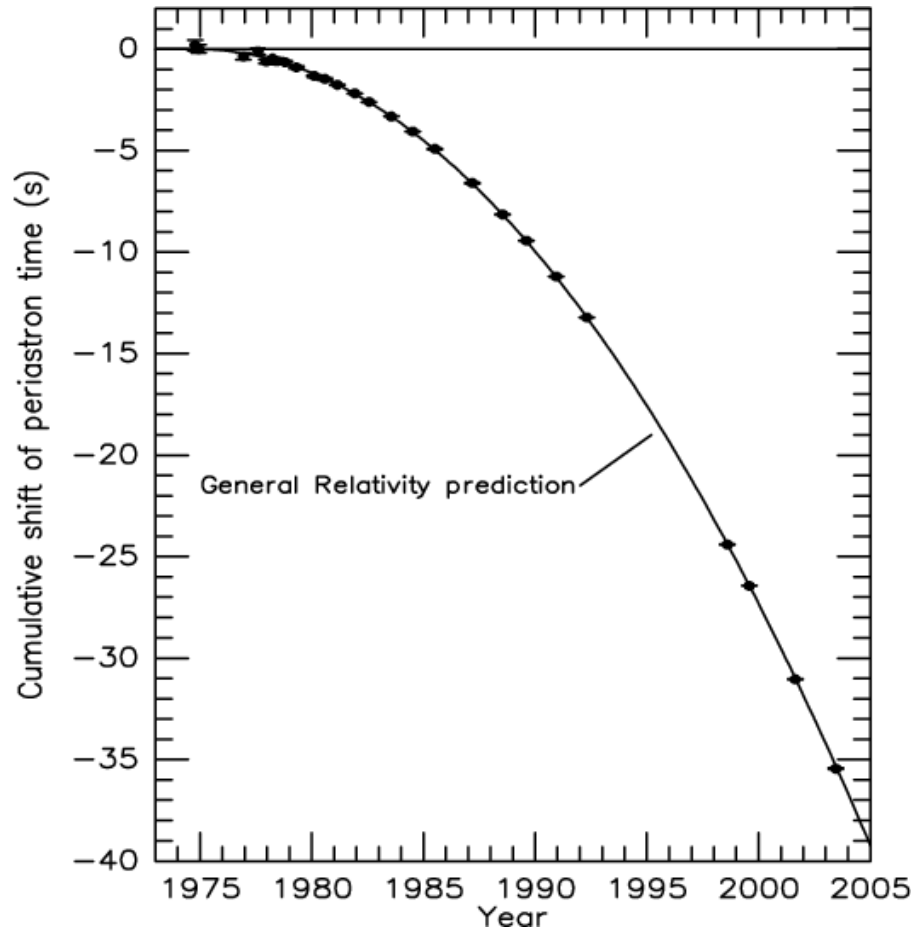
# The Masses of the Neutron Stars in the Binary Pulsar
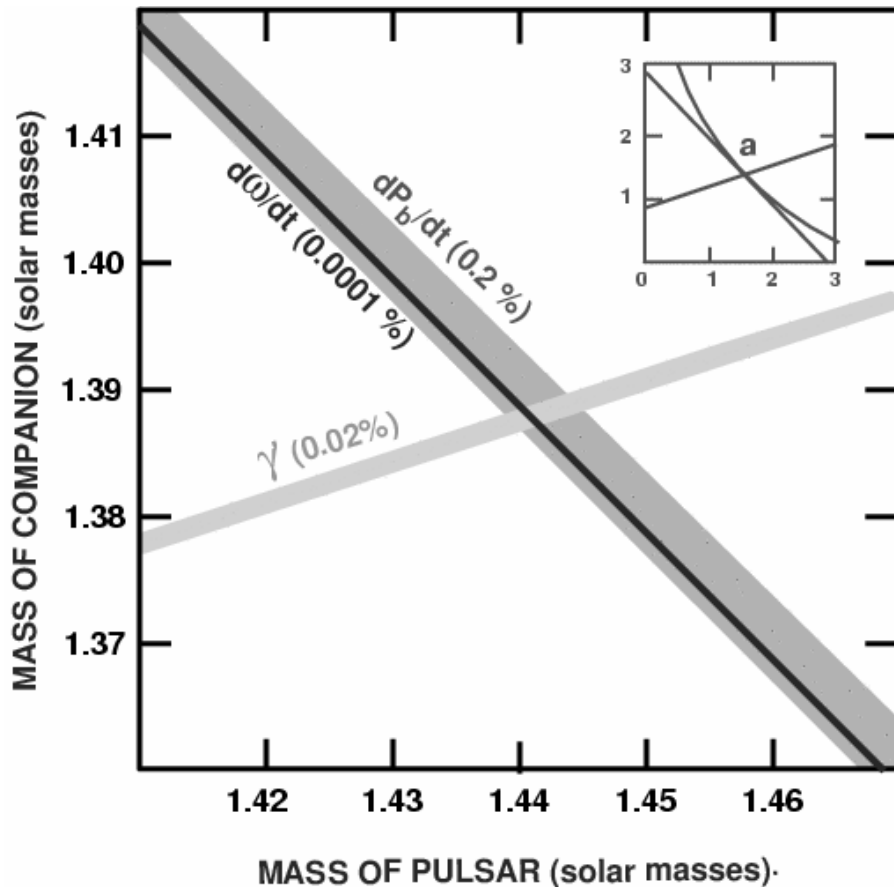
The width of each strip reflects the observational uncertainties in the timing measurements, shown as a percentage. The inset shows the same three most accurate constraints on the full mass plane; the intersection region has been magnified 400 times in the full figure. If General Relativity were not the correct theory of gravity, the lines would not intersect at one point.

Gravitational Radiation of the Binary Pulsar

The binary pulsar emits gravitational radiation and so leads to a speeding up of the stars in the binary orbit. The diagram shows the change of orbital phase as a function of time for the binary neutron star system PSR 1913+16 compared with the expected changes due to gravitational radiation energy loss by the binary system. These observations enable many alternative theories of gravity to be excluded.
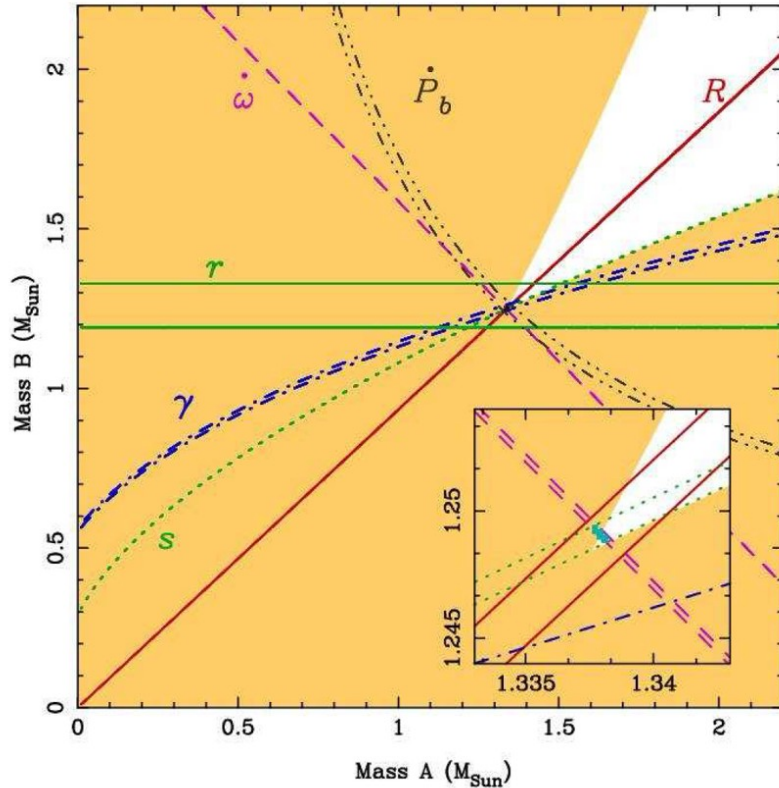
Double Pulsar System PSR J0737-3039
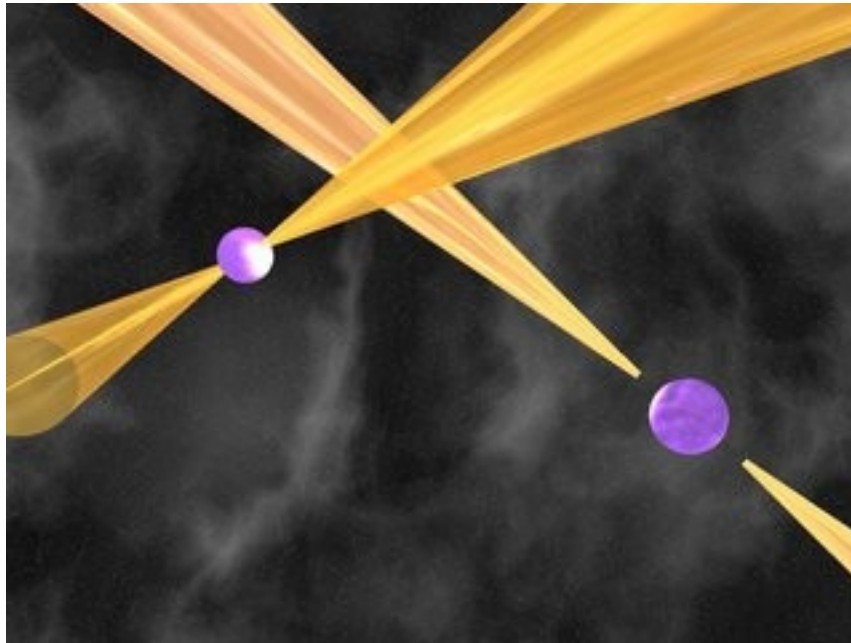
The first double pulsar system was discovered in 2003. Currently the double pulsar enables General Relativity to be tested at the 0.01% level.

	Pulsar A	Pulsar B
Spin period	23 msec	2.8 sec
Mass	1.337 $M_\odot$	1.250 $M_\odot$
Orbital period	2.4 hours	

Binary Pulsar J0737-3039

J0737-3039 is an even closer binary neutron star system in which both stars are pulsars. Therefore, their orbits can be determined more precisely. In 2.5 years, the precision with which General Relativity can be tested has approached that of PSR 1913+16.

| PK parameter	Observed	GR expectation	Ratio
$\dot{P}_{\mathrm{b}}$	1.252(17)	1.24787(13)	1.003(14)
γ (ms)	0.3856(26)	0.38418(22)	1.0036(68)
s	0.99974(−39,+16)	0.99987(−48,+13)	0.99987(50)
$r(\mu s)$	6.21(33)	6.153(26)	1.009(55)

Variation of the Gravitational Constant with Cosmic Epoch

Various solar system, astrophysical and cosmological tests can be made to find out if the gravitational constant has varied over cosmological time-scales.

Method	$(\dot{G}/G)/10^{-13}$ year^{-1}
Lunar laser ranging	4 ± 9
Binary pulsar PSR 1913+16	40 ± 50
Helioseismology	0 ± 16
Big Bang nucleosynthesis	0 ± 4

For binary pulsar data, the bounds are dependent upon the theory of gravity in the strong-field regime and on the neutron star equation of state. Big-bang nucleosynthesis bounds assume specific form for time dependence of G. There can have been little variation in the value of the gravitational constant over the last 10^{10} years.

Variation of the Fine Structure Constant with Cosmic Epoch
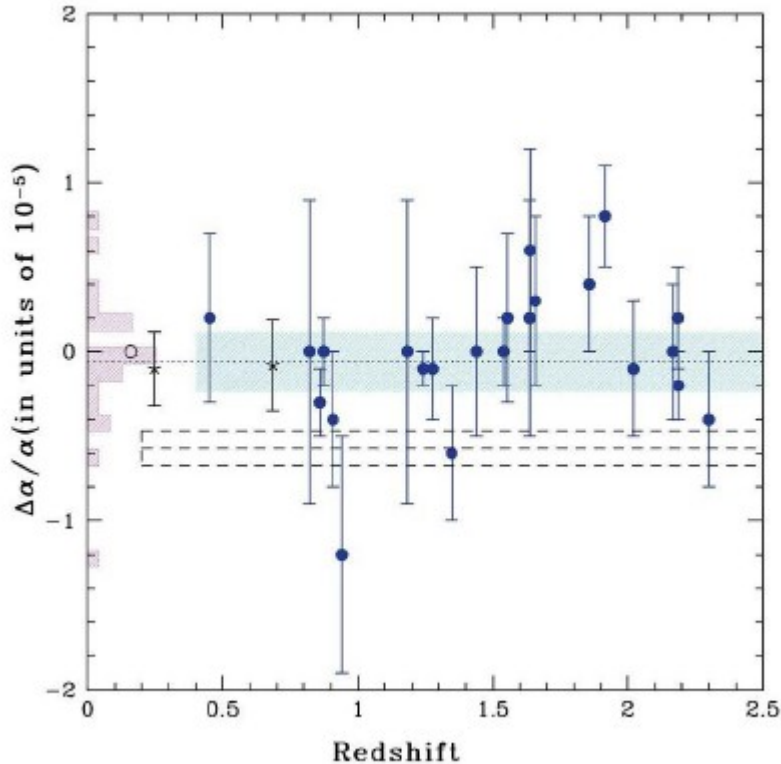
There has been some debate about whether or not the fine-structure constant α has changed very slightly with cosmic epoch from observations of fine-structure lines in large redshift absorption line systems in quasars. The Australian observers reported a small decrease in the value of α, shown by the open rectangle. The ESO observers found little evidence for changes.

The Growth of Small Density Perturbations

The standard equations of gas dynamics for a fluid in a gravitational field consist of three partial differential equations which describe (i) the conservation of mass, or the equation of continuity, (ii) the equation of motion for an element of the fluid, Euler's equation, and (iii) the equation for the gravitational potential, Poisson's equation.

$$\text{Equation of Continuity}\;:\;\; \frac{\partial \varrho}{\partial t} + \nabla \cdot (\varrho v) = 0 \; ;$$

$$\text{Equation of Motion}\;:\;\; \frac{\partial v}{\partial t} + (v \cdot \nabla)v = -\frac{1}{\varrho}\nabla p - \nabla \phi \; ;$$

$$\text{Gravitational Potential}\;:\;\; \nabla^2 \phi = 4\pi G \varrho \; .$$

These equations describe the dynamics of a fluid of density ρ and pressure p in which the velocity distribution is **v**. The gravitational potential φ at any point is given by Poisson's equation in terms of the density distribution ρ.

The Growth of Small Density Perturbations

We perturb the system about the uniform expansion $v = H_0 r$:

$$v = v_0 + \delta v, \quad \varrho = \varrho_0 + \delta\varrho, \quad p = p_0 + \delta p, \quad \phi = \phi_0 + \delta\phi.$$

After a bit of algebra, we find the following equation for the peculiar velocity induced by the growth of the perturbation:

$$\frac{\mathrm{d}}{\mathrm{d}t}\left(\frac{\delta\varrho}{\varrho_0}\right) = \frac{\mathrm{d}\Delta}{\mathrm{d}t} = -\nabla \cdot \delta v,$$

where $\Delta = \delta\varrho/\varrho_0$ is the density contrast. After a little more algebra, we obtain the wave equation for Δ

$$\frac{\mathrm{d}^2\Delta}{\mathrm{d}t^2} + 2\left(\frac{\dot{a}}{a}\right)\frac{\mathrm{d}\Delta}{\mathrm{d}t} = \Delta(4\pi G\varrho_0 - k^2 c_{\mathsf{s}}^2),$$

where the adiabatic sound speed c_{s}^2 is given by $\partial p/\partial\varrho = c_{\mathsf{s}}^2$ and k is the proper wavevector.

The Jeans' Instability in an Expanding Medium

The Einstein–de Sitter Critical Model $\Omega_0 = 1$. In this case, $4\pi G\varrho = 2/3t^2$, $\dot{a}/a = 2/3t$ and we find the key result

$$\Delta = \frac{\delta\varrho}{\varrho} \propto (1+z)^{-1}.$$

The growth of the perturbation in the case of the critical Einstein–de Sitter universe is *algebraic*.

The Empty, Milne Model $\Omega_0 = 0$ In this case,

$$\varrho = 0 \qquad \text{and} \qquad \frac{\dot{a}}{a} = \frac{1}{t},$$

and Δ = constant.

In the early stages of the matter-dominated phase, the dynamics of the world models tend to $a \propto t^{2/3}$, and the density contrast grows linearly with a. At redshifts $\Omega_0 z \ll 1$, the amplitudes of the perturbations grow very slowly.

# Models with $\Omega_\Lambda = 0$
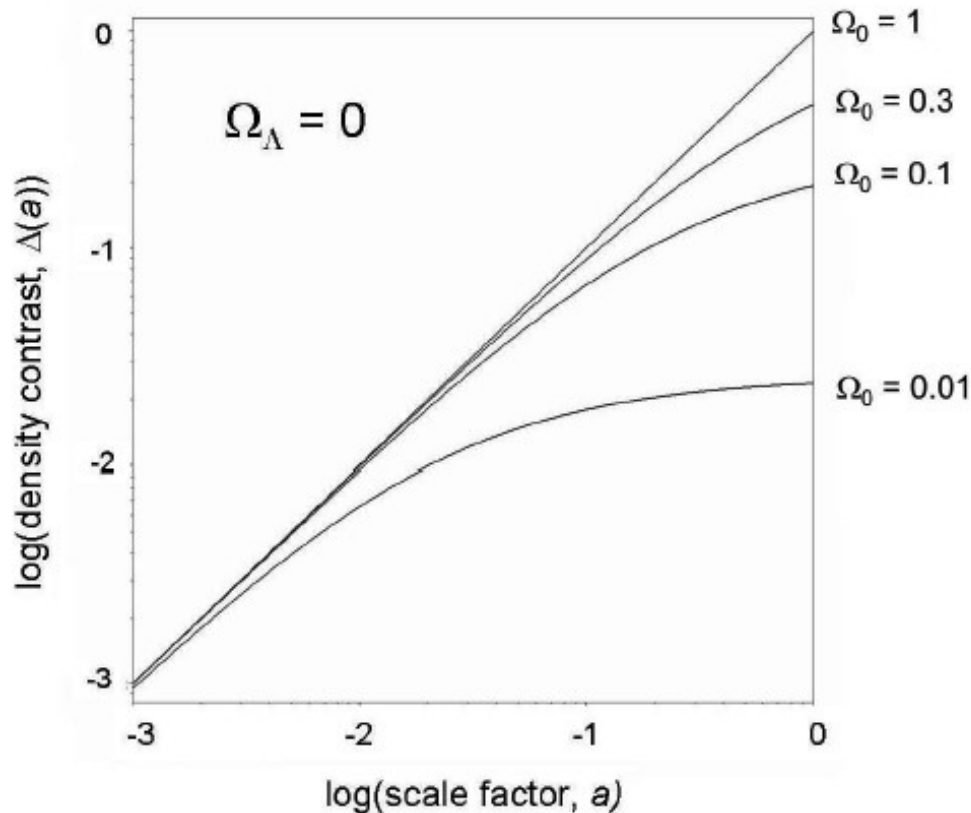
The development of density fluctuations from a scale factor $a = 1/1000$ to $a = 1$ are shown for a range of world models with $\Omega_\Lambda = 0$. These results are consistent with the calculations carried out above, in which it was argued that the amplitudes of the density perturbations vary as $\Delta \propto a$ so long as $\Omega_0 z \gg 1$, but the growth essentially stops at smaller redshifts.

Models with finite Ω_Λ
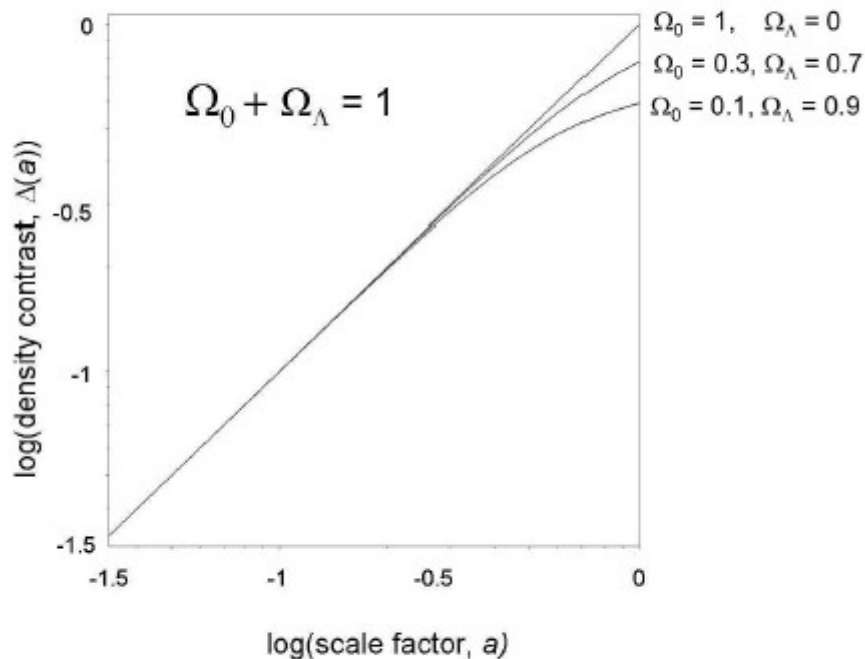
The models of greatest interest are the flat models for which $(\Omega_0 + \Omega_\Lambda) = 1$, in all cases, the fluctuations having amplitude $\Delta = 10^{-3}$ at $a = 10^{-3}$. The growth of the density contrast is somewhat greater in the cases $\Omega_0 = 0.1$ and 0.3 as compared with the corresponding cases with $\Omega_\Lambda = 0$. The fluctuations continue to grow to greater values of the scale-factor a, corresponding to smaller redshifts, as compared with the models with $\Omega_\Lambda = 0$.

The Harrison–Zeldovich Power Spectrum
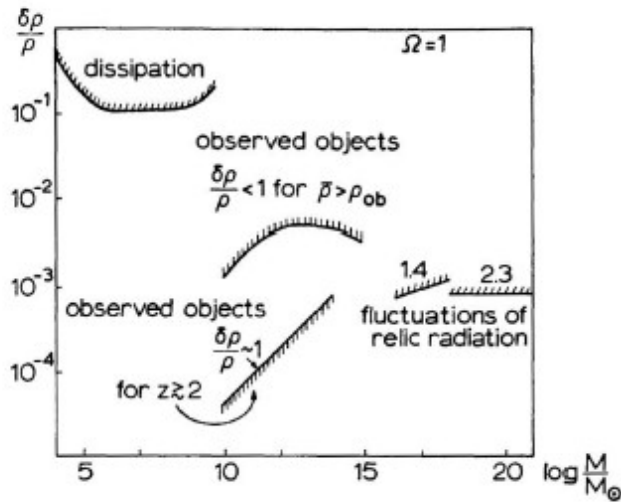
The constraints on the form of the perturbation spectrum in 1971 derived by Sunyaev and Zeldovich.

They put in what was needed to produce the observed structures today.

Sunyaev and Zeldovich used a variety of constraints to derive the form of the initial power-spectrum of density perturbations as they came through the horizon. They found a scale-invariant spectrum $\delta\varrho/\varrho = 10^{-4}$ on mass scales from 10^5 to $10^{20} \, M_\odot$.

Harrison studied the form the primordial spectrum must have in order to prevent the overproduction of excessively large amplitude perturbations on small and large scales. A power spectrum of the form

$$P(k) \propto k$$

does not diverge on large physical scales and so is consistent with the observed large-scale isotropy of the Universe. Run simulation.

Confrontation with Observation

The revolution of the last 10 years has been the remarkable agreement between completely independent approaches to estimating basic cosmological parameters.

- Supernovae of Type 1A

- Fluctuation spectrum and polarisation of the Cosmic Microwave Background Radiation

- The power spectrum of galaxies from the Sloan Digital Sky Survey and the AAO 2dF galaxy survey.

- Mass density of the Universe from the infall velocities of galaxies into large scale structures.

- The formation of the light elements by primordial nucleosynthesis.

- Cosmic time scale from the theory of stellar evolution and nucleocosmochronology.

- The value of Hubble's constant from the HST Key Project.

- The statistics of gravitational lenses.

Supernovae of Type 1a
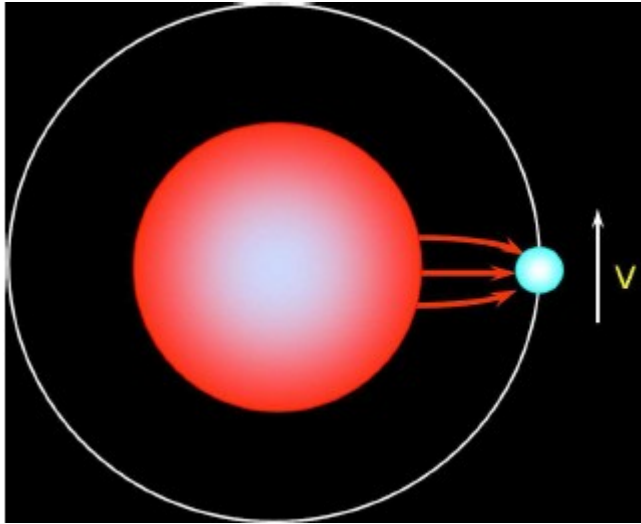
The Type 1a supernovae are associated with the explosions of white dwarfs in binary systems, probably because of a nuclear deflagration associated with mass transfer from the companion onto the surface of the white dwarf.

Type 1a supernovae have dominated methods for extending the redshift-distance relation to large redshifts. They are brightest supernovae and are observed to have remarkably standard properties, particularly when corrections are made for the luminosity-width relation.
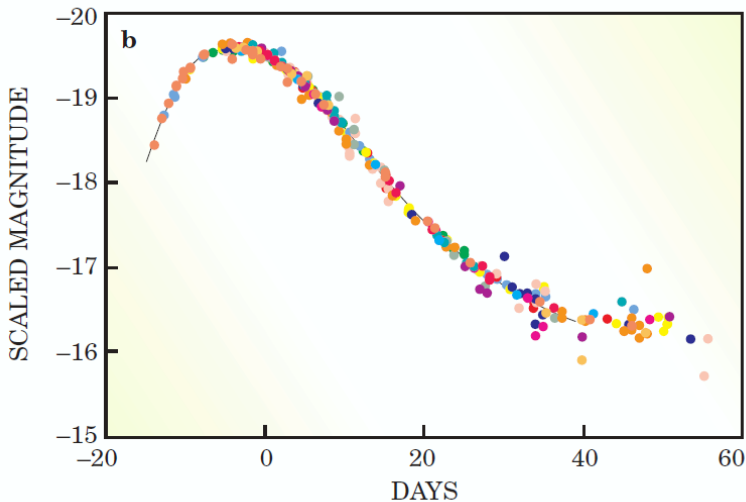
The Accelerating Universe
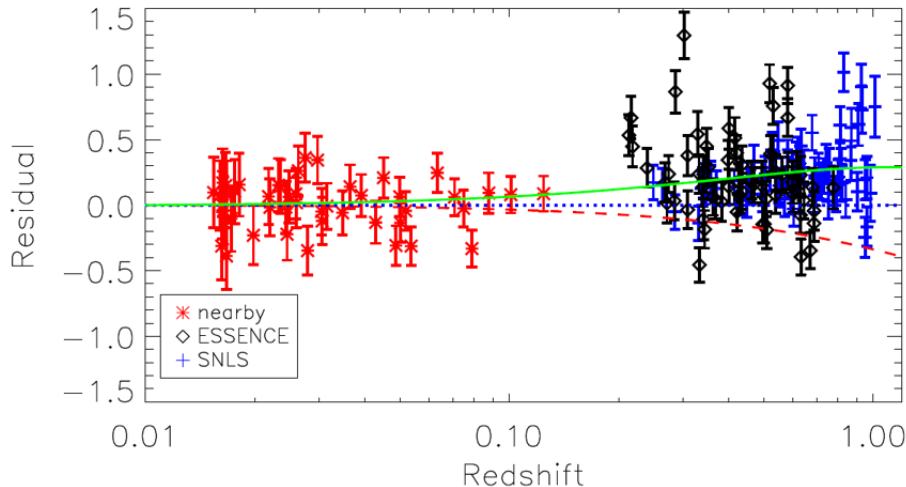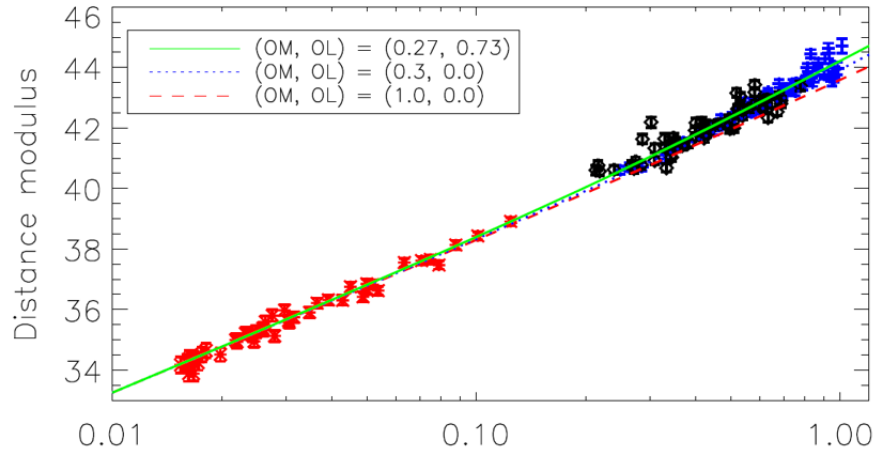
The ESSENCE project has the objective of measuring the redshifts and distances of about 200 supernovae. The Supernova Legacy Project aims to obtain distances for about 500 supernovae. The observations are consistent with a finite and positive value of the cosmological constant. The green line and residuals are for a CDM model with $\Omega_0 = 0.27$ and $\Omega_\Lambda = 0.73$ (Wood-Vasey et al., 2007).

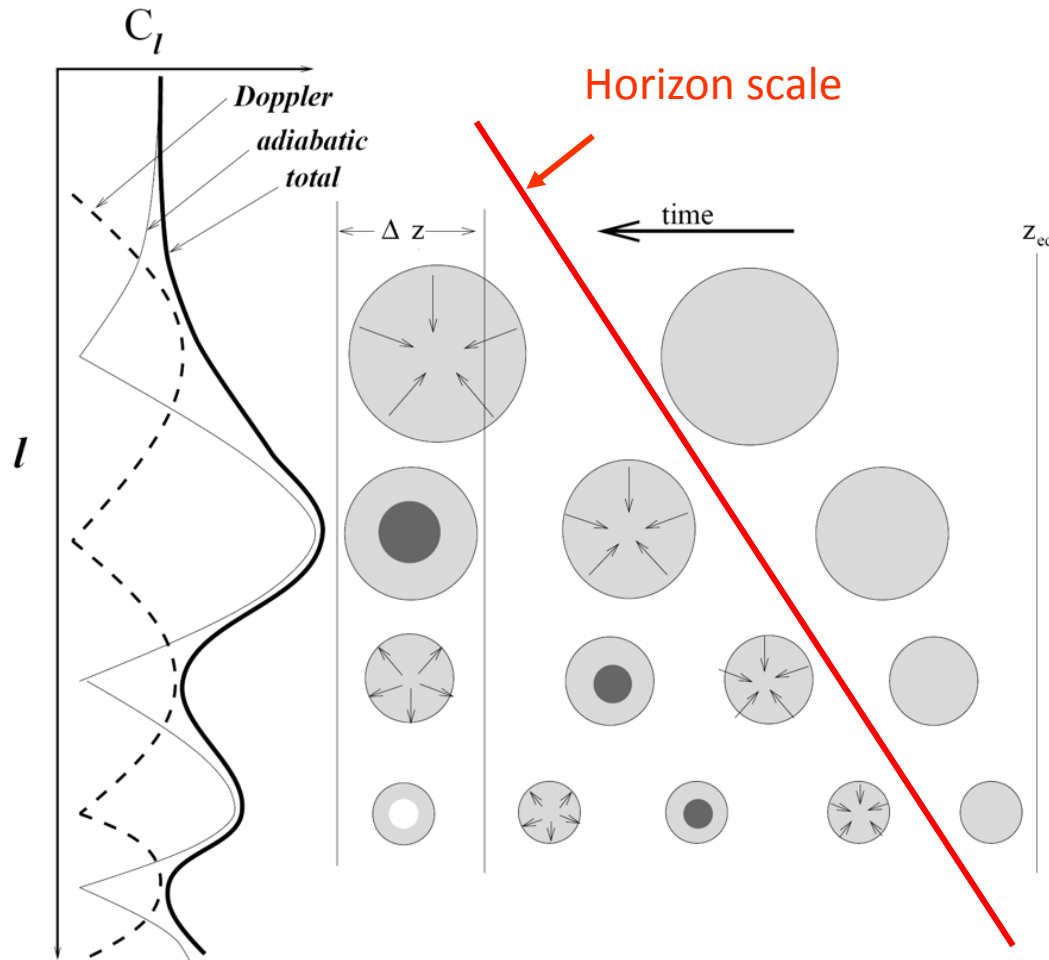# The Origin of the COBE Fluctuations

The importance of the COBE fluctuations is that they are the fingerprints of the formation of the largest scale structures on the last scattering surface.
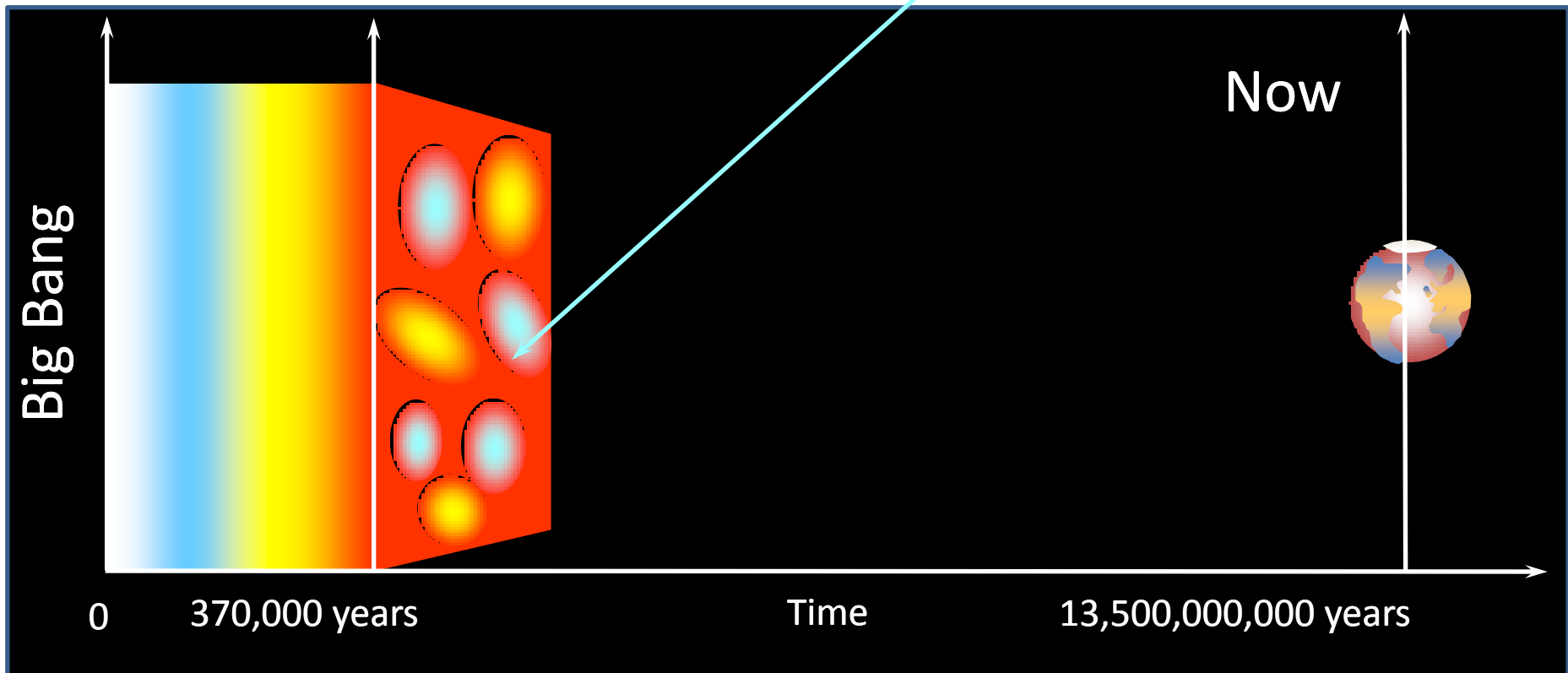
# Predicted Power-spectrum of Fluctuations in Cosmic Microwave Background Radiation
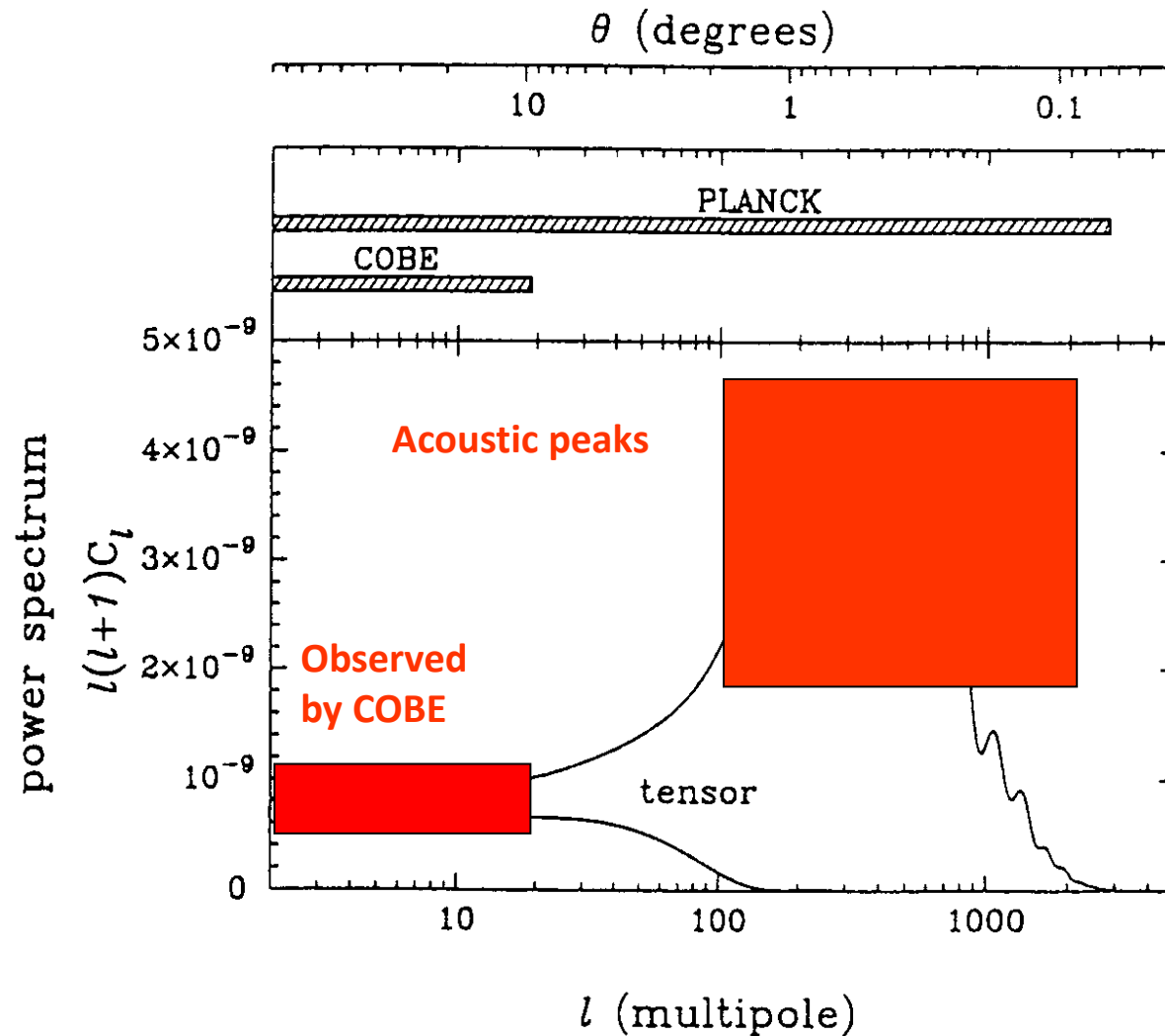
Origin of the Acoustic Peaks

All perturbations have scales greater than the cosmological horizon r_H = ct early enough in the Universe. When they come through the horizon the baryonic perturbations become sound waves and their amplitude at the last scattering surface depends on the phase of the waves at that time.
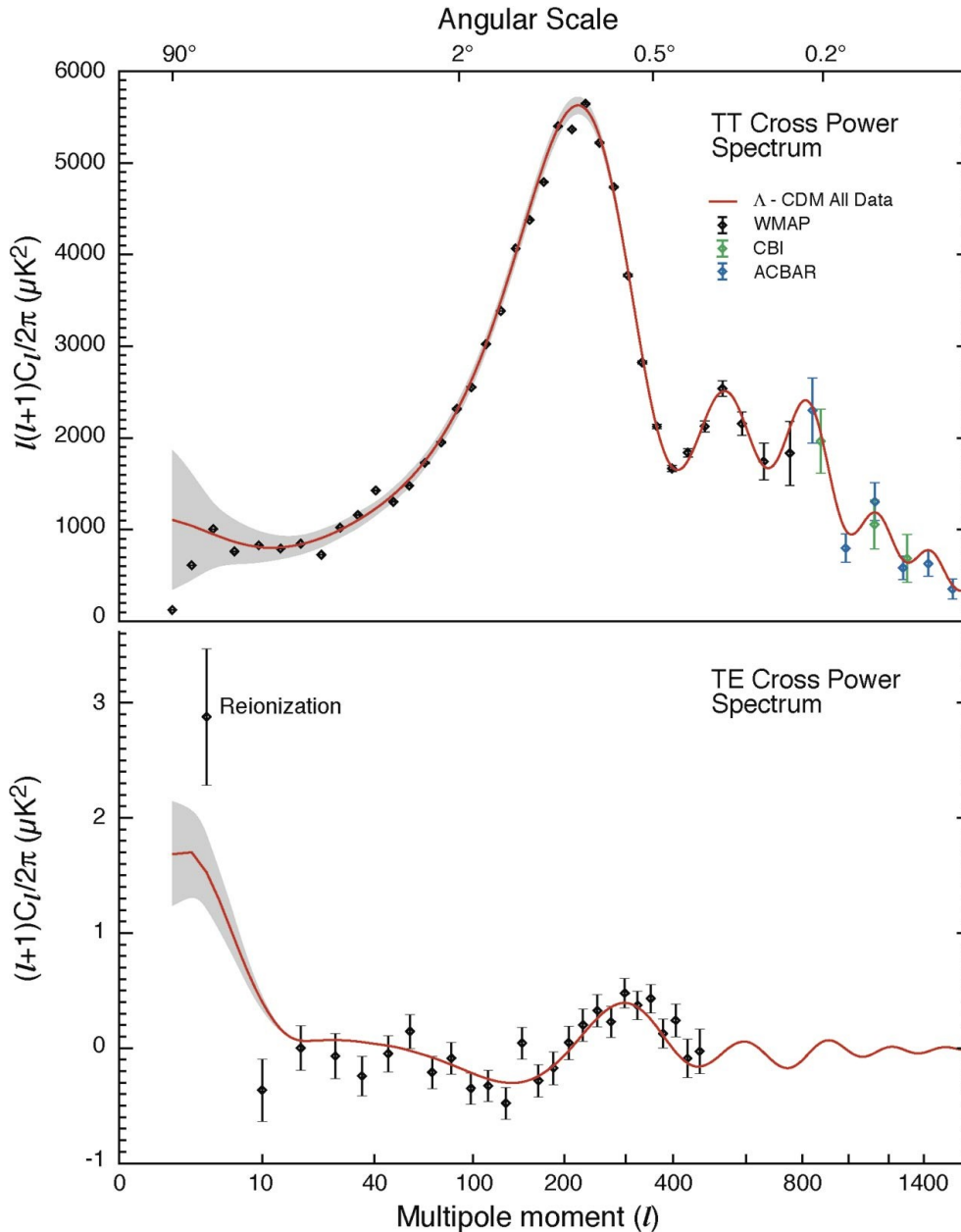
Wilkinson Microwave Anisotropy Probe (WMAP)
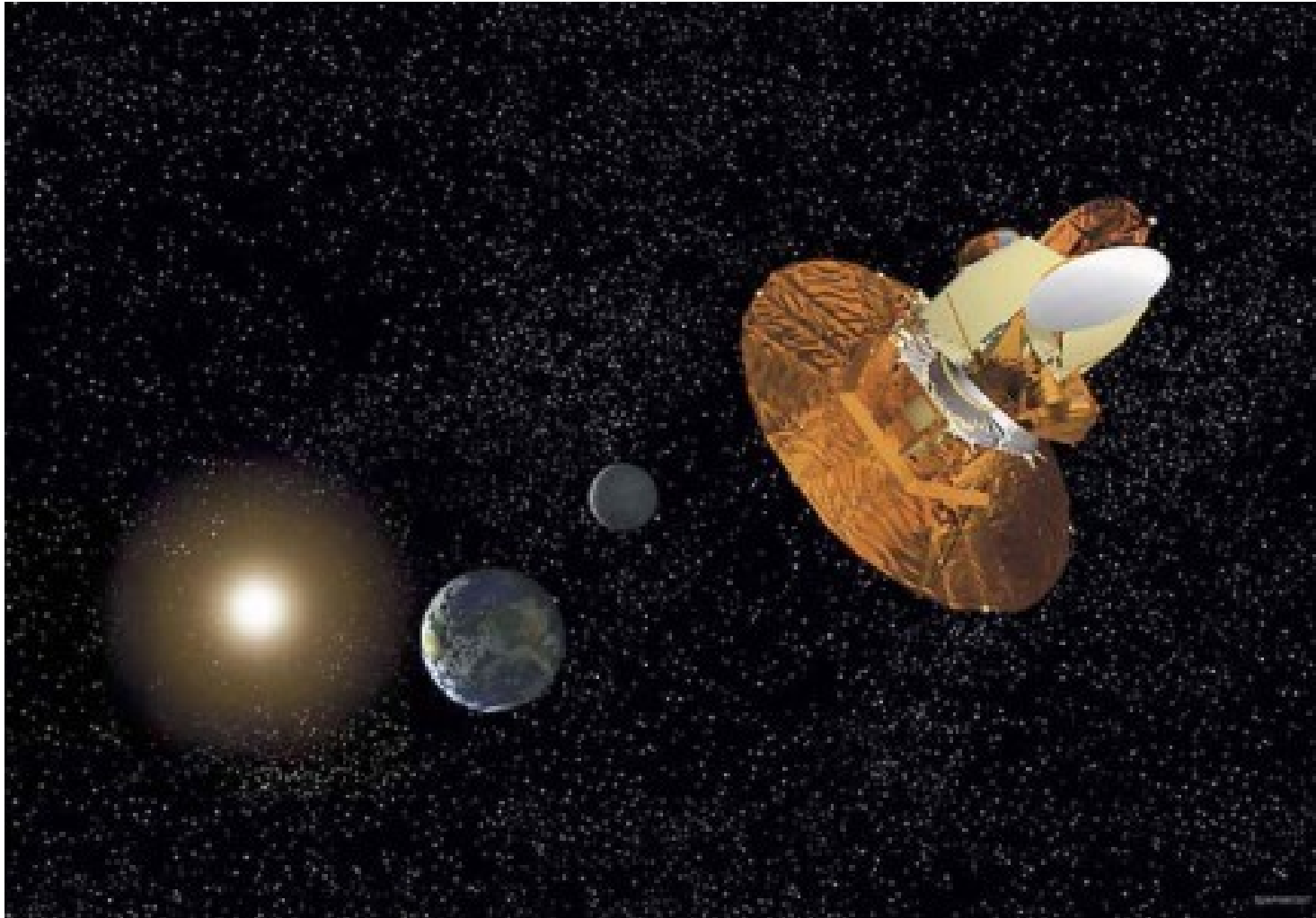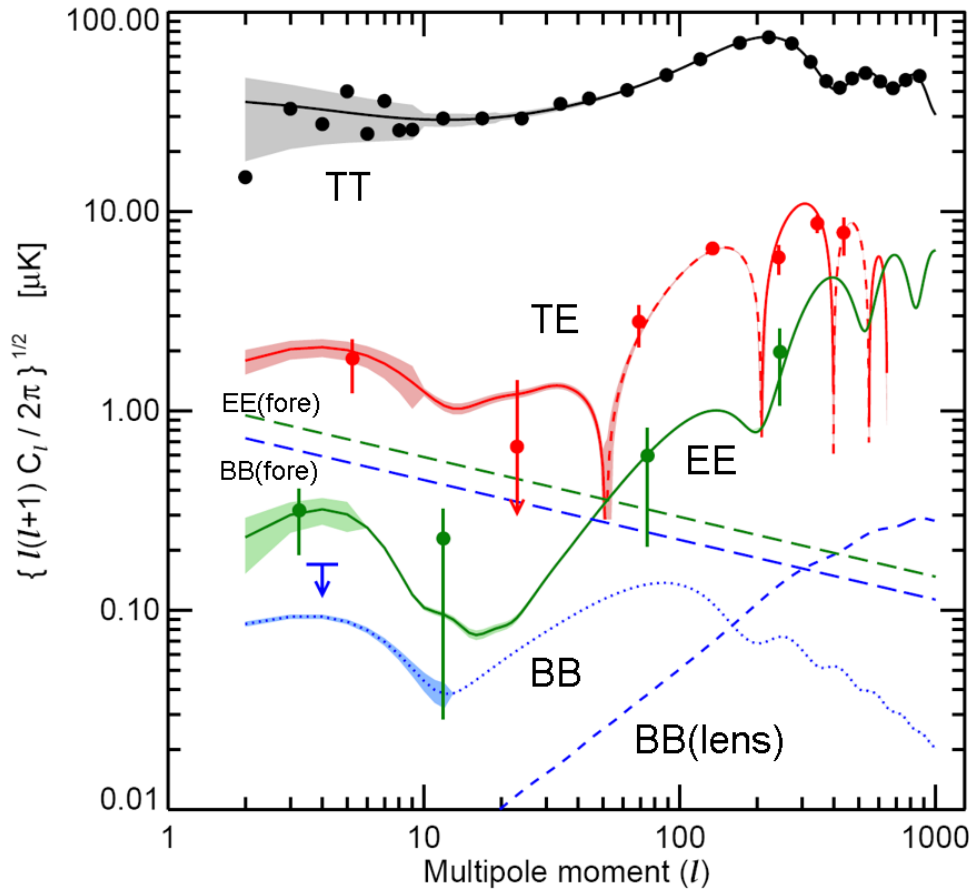

Launched 30 June 2001
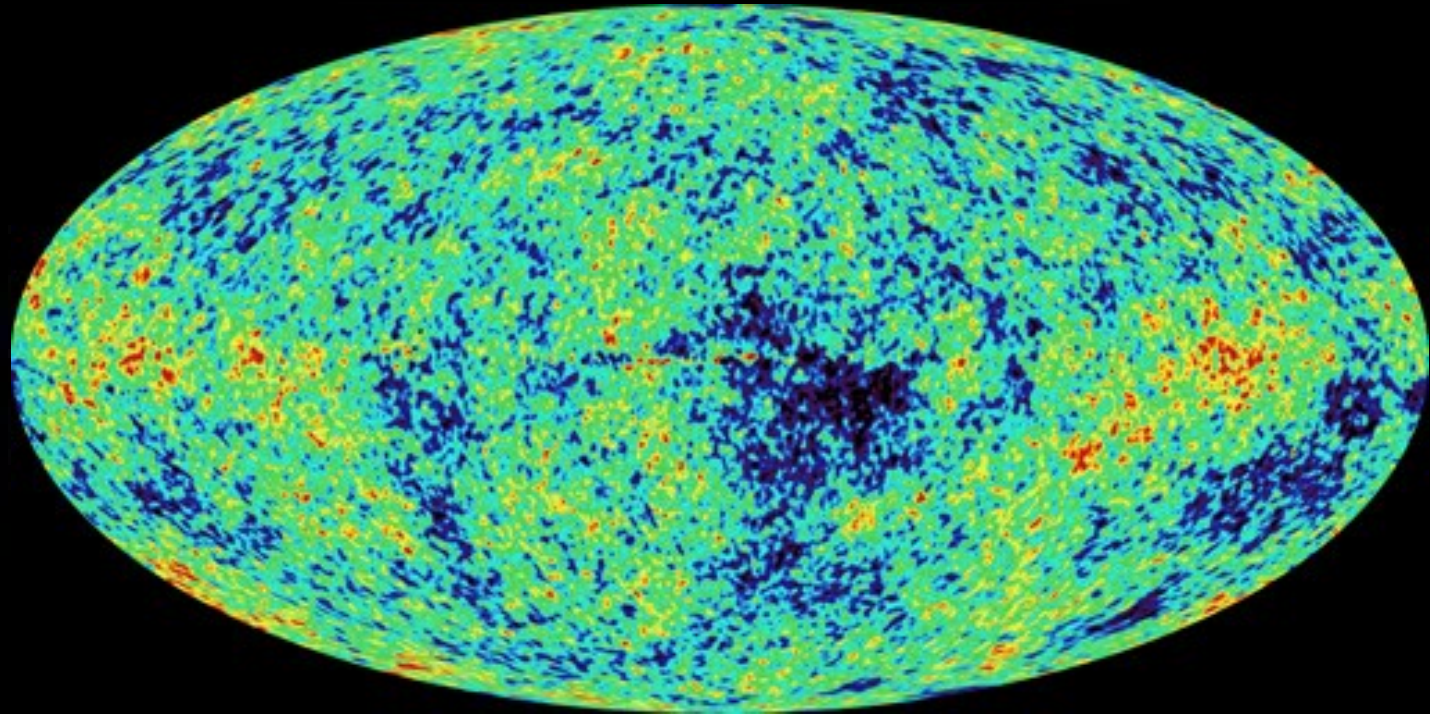
WMAP Image of the Sky

WMAP Power spectrum 1-year data

- Spectacular agreement with "vanilla" ΛCDM model.

- Possible lower amplitude at low values of *l*

- Cross-correlation of polarisation with scalar amplitudes of power spectrum agrees with predictions of pure scalar field with early reionisation.

WMAP Power Spectrum 3-year Data

- Again spectacular agreement with "vanilla" ΛCDM model.

- Note important reionisation signature

- Note limits to primordial gravitational waves.

Our Universe – Its Properties

## Densities relative to the critical density

- The geometry of the Universe is flat: $\Omega_0 + \Omega_\Lambda \approx 1$.

- 72% of the mass-energy of the Universe is in the form of dark energy: $\Omega_\Lambda \approx 0.72$.

- 23% of the mass of the Universe is in the form of cold dark matter: $\Omega_D \approx 0.23$.

- 5% of the Universe is in the form of ordinary matter $\Omega_B \approx 0.05$.

- Hubble's constant: $H_0 = 72 \pm 7 \ (1\sigma) \ \text{km s}^{-1} \ \text{Mpc}^{-1}$

Longer List of Cosmological Parameters

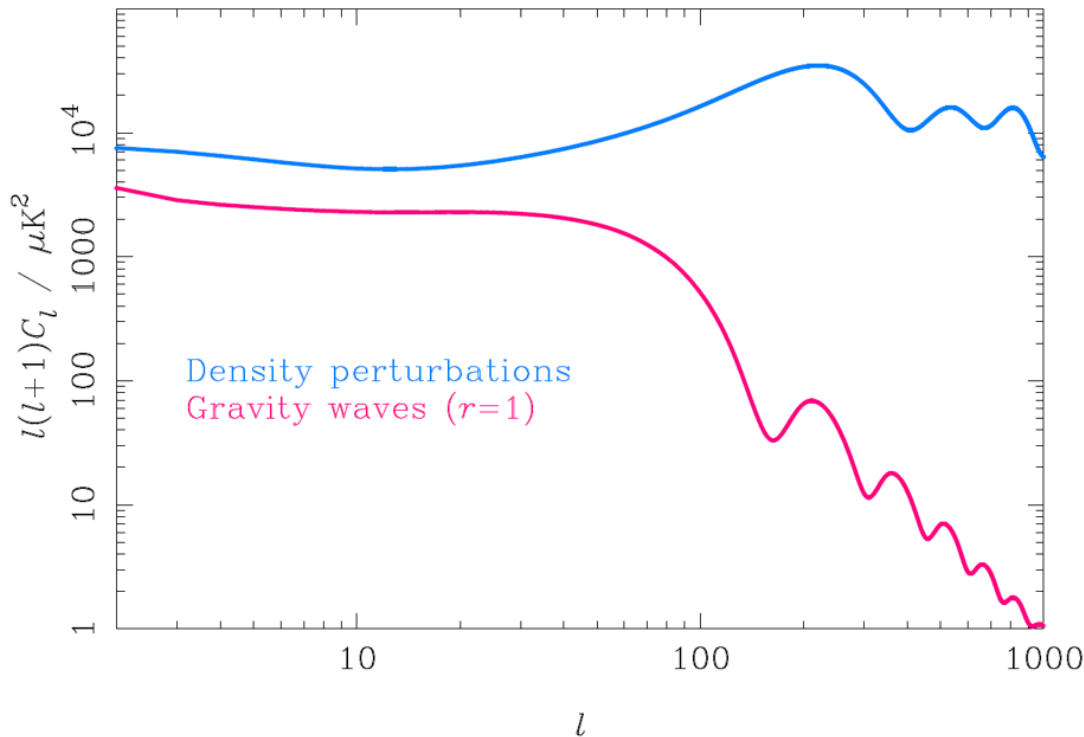| Parameter	Definition
$\omega_B = \Omega_B h^2$	baryon density parameter
$\omega_D = \Omega_D h^2$	cold dark matter density parameter
h	Hubble's constant
Ω_Λ	dark energy density parameter
n_S	scalar spectral index — Standard value = 1
τ	reionisation optical depth
σ_8	density variance in 8 Mpc spheres
w	dark energy equation of — Standard value = -1
Ω_k	curvature density parameter
$f_\nu = \Omega_\nu / \Omega_D$	massive neutrino fraction — Standard value = 0
N_ν	number of relativistic neu — Standard value = 3
$\Delta_{\mathcal{R}}^2$	amplitude of curvature perturbations
r	tensor-scalar ratio
A_S	amplitude of scalar power-spectrum
$\alpha = d \ln K / d \ln k$	running of scalar spectra — Standard value = 0
A_{SZ}	SZ marginalization factor
b	bias factor
z_S	weak lensing source redshift

Planck and the Cosmic Microwave Background Radiation
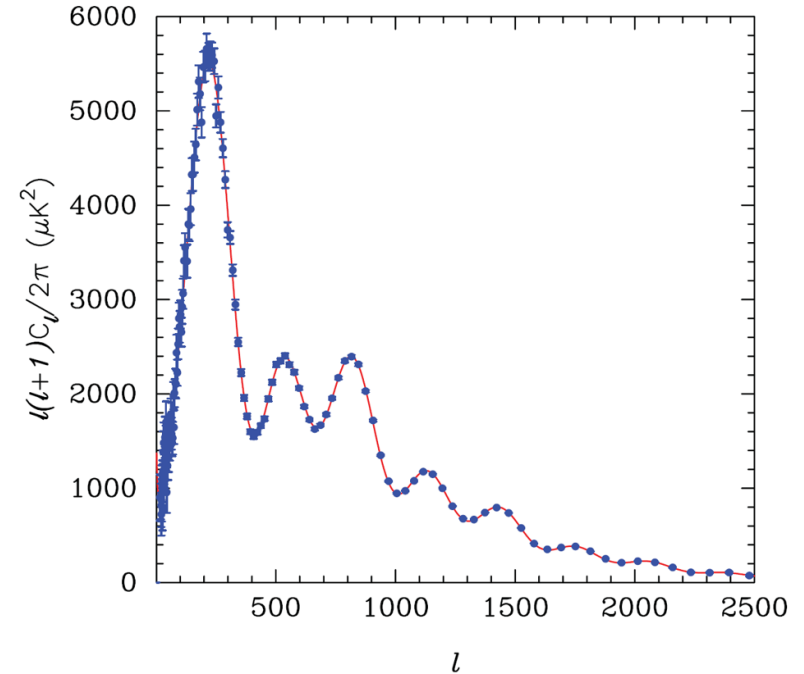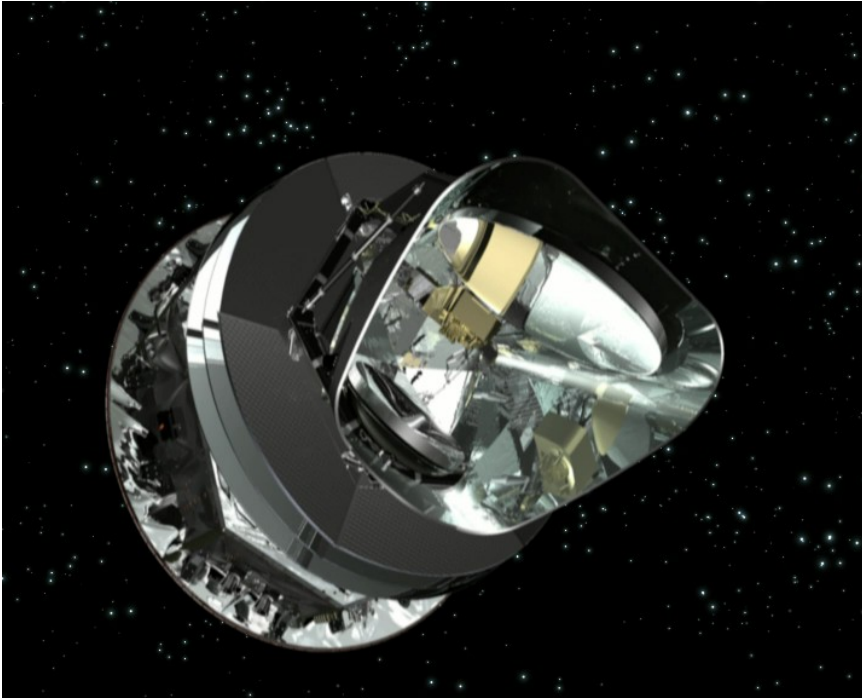
Planck will result in roughly an order of magnitude improvement in precision in CMB studies.

Planck and the Cosmic Microwave Background Radiation

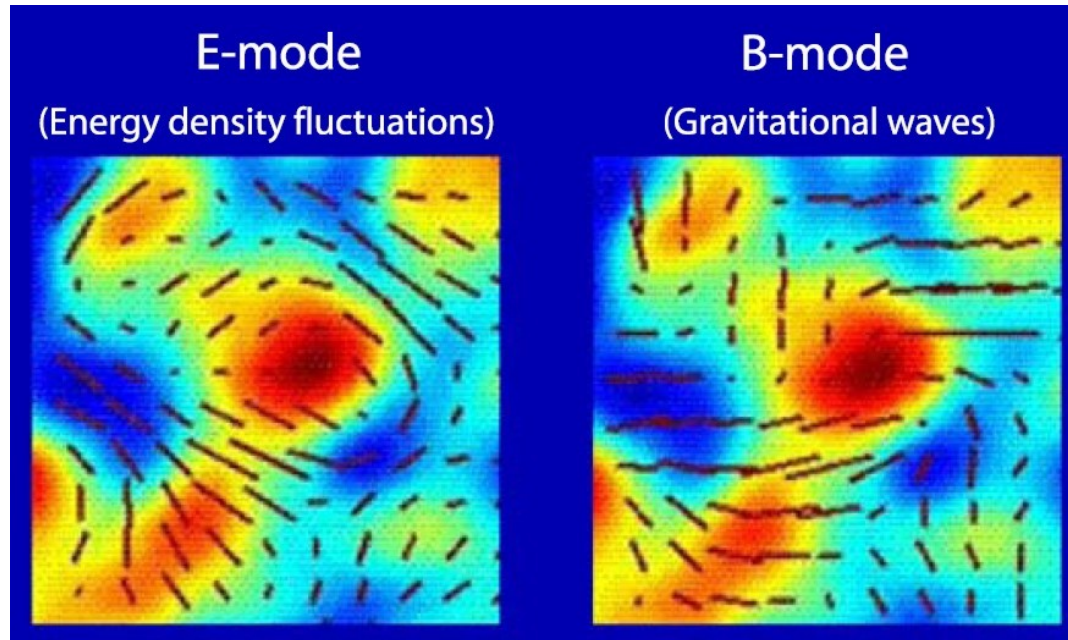The Planck one-year all-sky survey

(c) ESA, HFI and LFI consortia, July 2010
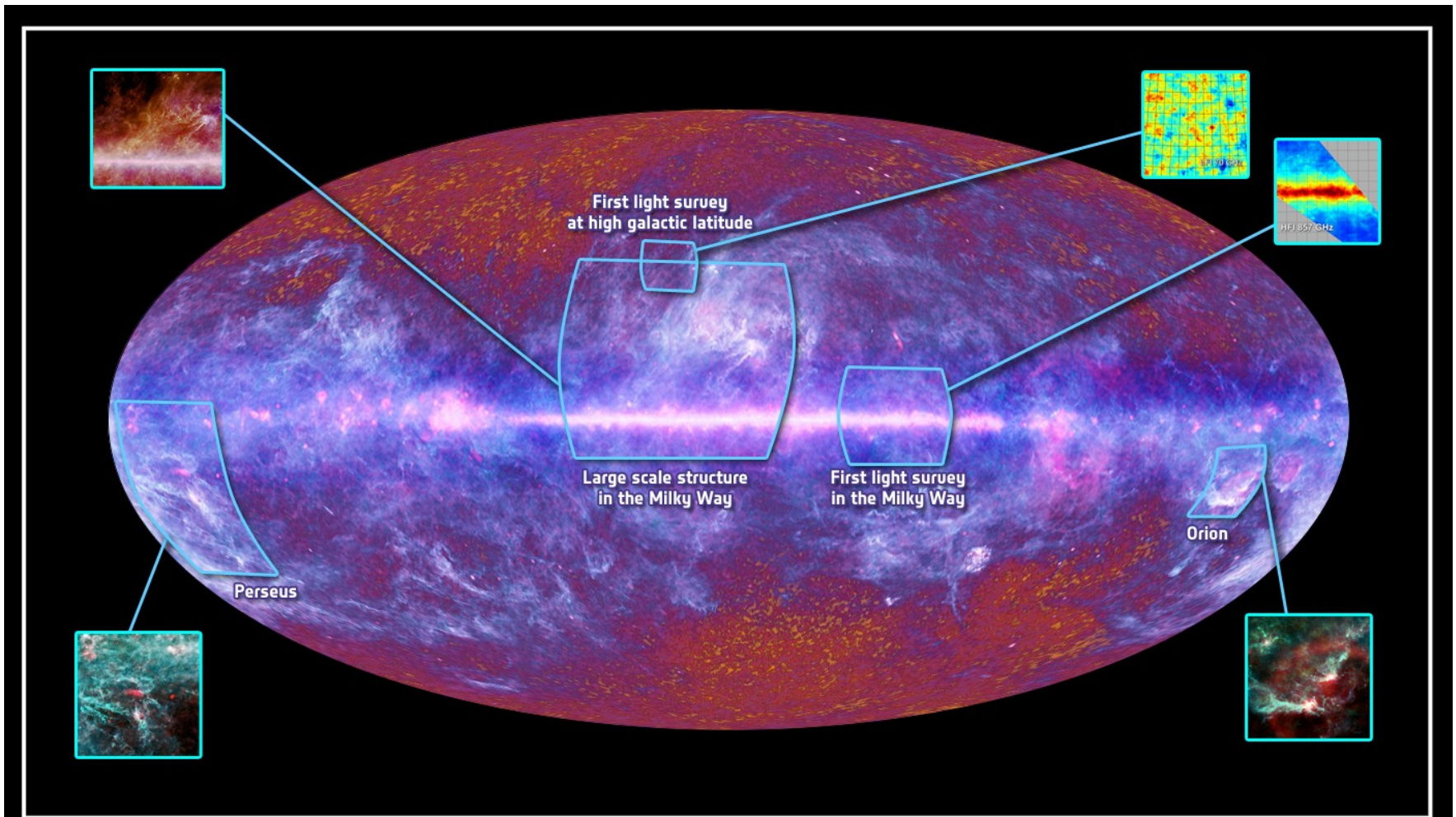
The Power Spectrum of Scalar and Tensor Perturbations

Density perturbations
Gravity waves ($r=1$)

The detection of primordial gravitational waves would be one of the greatest achievements of observational cosmology

The Polarisation of the Cosmic Microwave Background Radiation

The scalar E-modes arise from simple density fluctuations. The B-modes arise from primordial gravitational waves. These need to be distinguished from B-modes from gravitational lensing.

Best Estimates of Hubble's Constant

The controversies of the 1970s and 1980s have been resolved thanks to a very large effort by many observers to improve knowledge of the distances to nearby galaxies.

Final result of HST key project

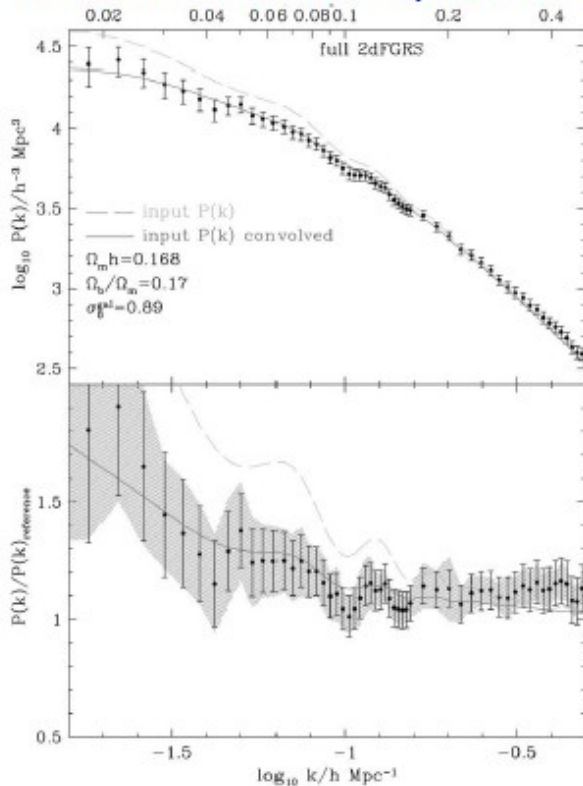$H_0 = 72 \pm 7\ (1\sigma)$ km s^{-1} Mpc^{-1}

Gravitational time delays

$H_0 = 68 \pm 6(\text{stat}) \pm 8\ (\text{syst})$ km s^{-1} Mpc^{-1}

Sunyaev-Zeldovich effect

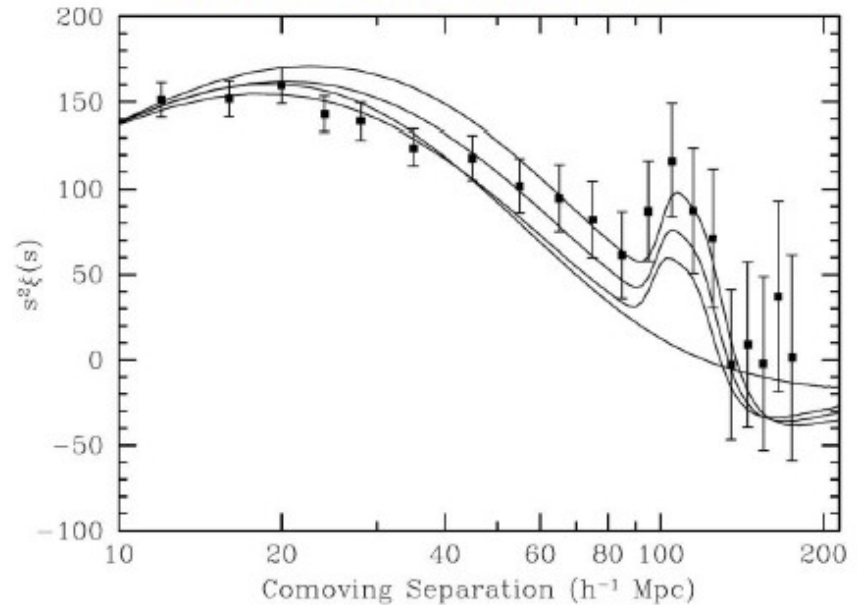$H_0 = 76.9 \pm 4(\text{stat}) \pm 9\ (\text{syst})$ km s^{-1} Mpc^{-1}

Acoustic Peaks in the Galaxy Power-Spectra

The acoustic peaks in the distribution of galaxies at redshifts z ≤ 0.5 correspond to the temperature maxima in the power-spectrum of fluctuations in the Cosmic Microwave Background Radiation imprinted at z = 1000.

Average Mass Density in the Universe from Infall into Superclusters
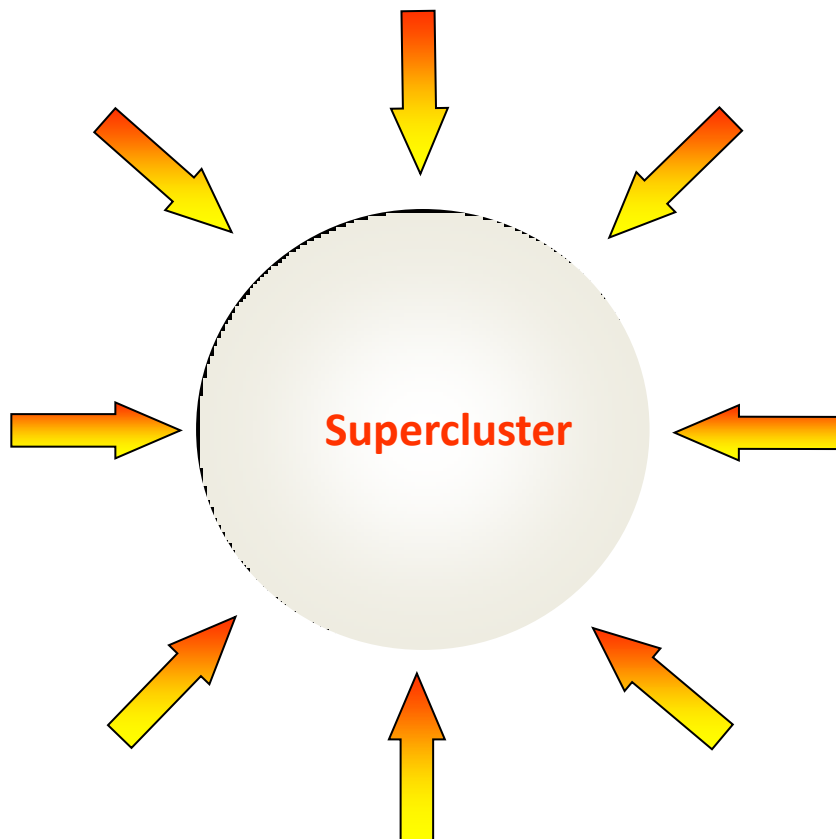
Radial
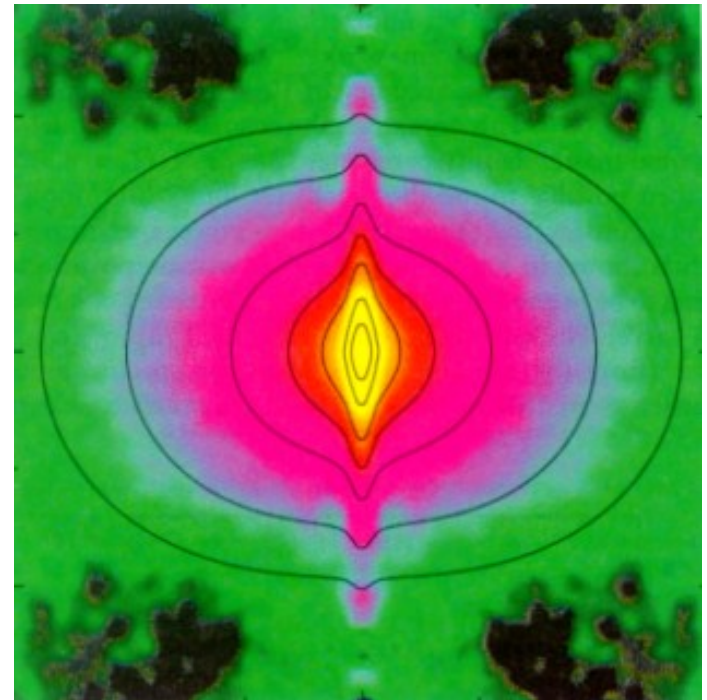
Supercluster

On sky

Infall of galaxies into superclusters provides an estimate of the average mass density on very large scales.

Average Mass Density in the Universe from Infall into Superclusters
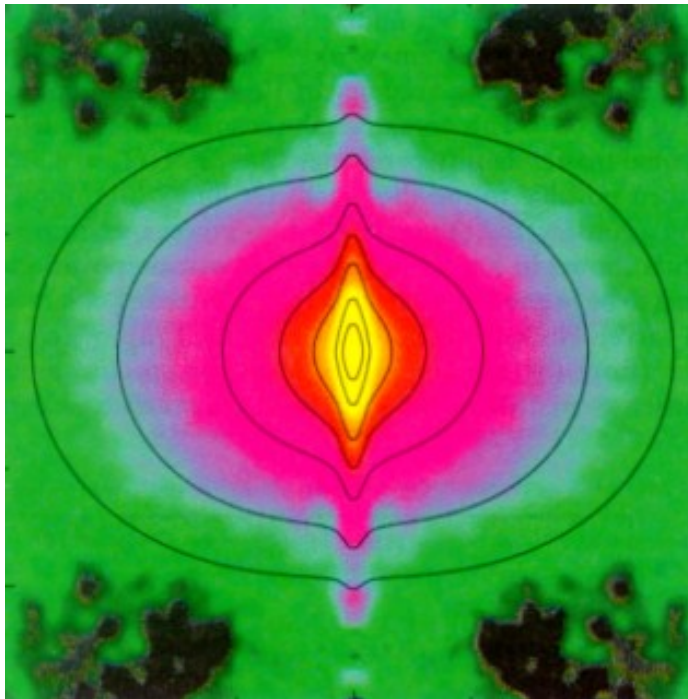
Radial

On sky

The two-dimensional correlation function for galaxies in the radial and transverse directions selected from the 2dF Galaxy Redshift Survey. The flattening in the vertical direction is due to the infall of galaxies into large-scale density perturbations. The elongations along the central vertical axis are associated with the velocity dispersion in clusters of galaxies. The inferred overall density parameter is $\Omega_0 = 0.25$.

Formation of the Light Elements by Primordial Nucleosynthesis
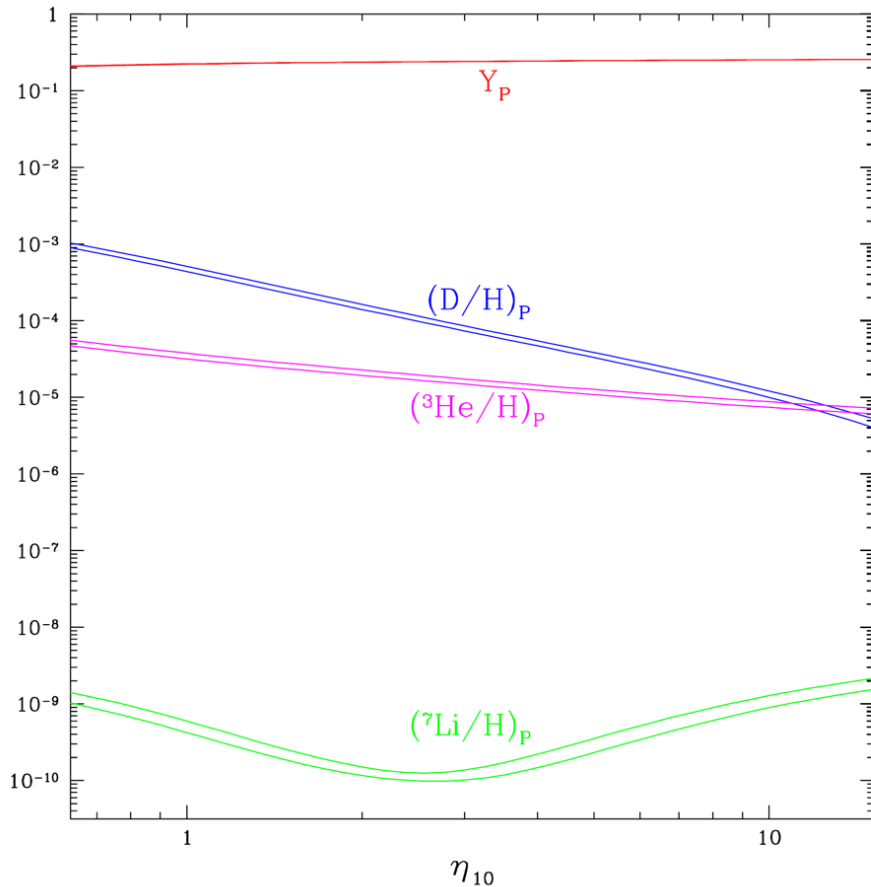
The predicted primordial abundances of the light elements as a function of the present baryon-to photon ratio in the form

$$\eta = 10^{10} n_{\mathrm{B}}/n_{\gamma} = 274\, \Omega_{\mathrm{B}} h^2$$

Yp is the abundance of helium by mass, whereas the abundances for D, ^{3}He and ^{7}Li are plotted as ratios by number relative to hydrogen.

Formation of the Light Elements by Primordial Nucleosynthesis

Helium
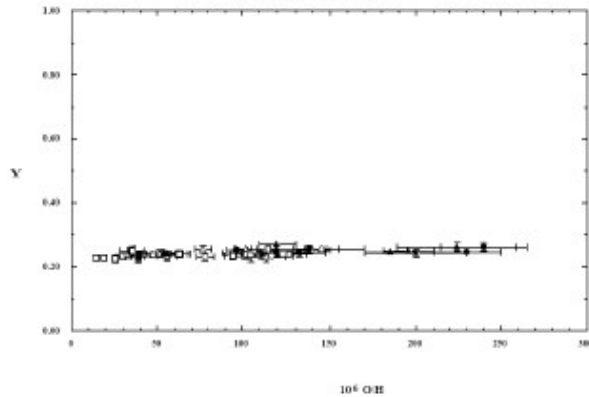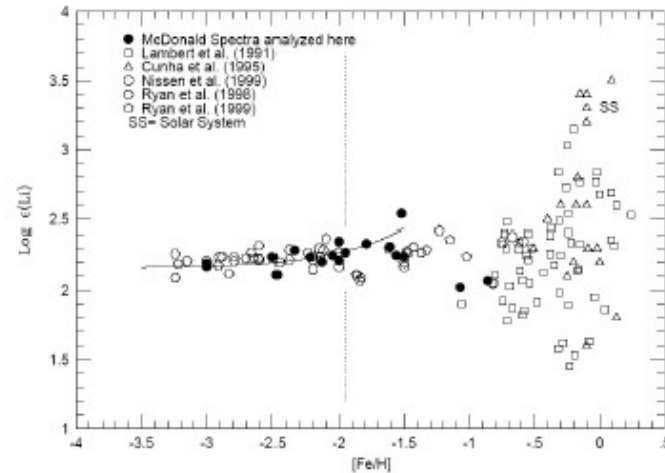
Deuterium

Lithium
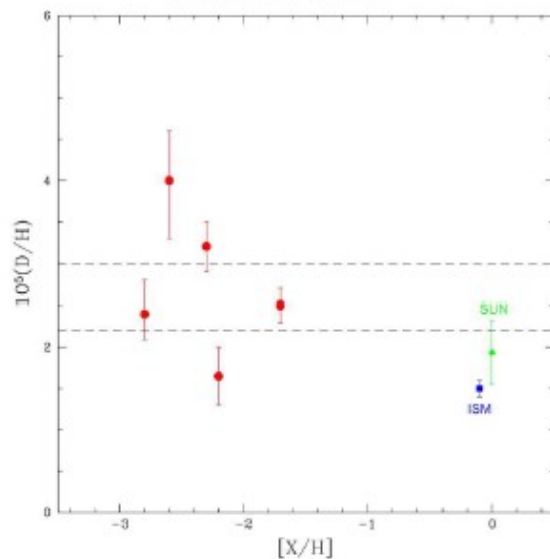
Steigman finds a best fitting value $\Omega_B h^2 = 0.022^{+0.003}_{-0.002}$. This can be compared with the independent estimate from the power-spectrum of fluctuations of the Cosmic Microwave Background Radiation $\Omega_B h^2 = 0.0224 \pm 0.0009$.

Cosmic Time-scales

The Ages of the Oldest Globular Clusters:
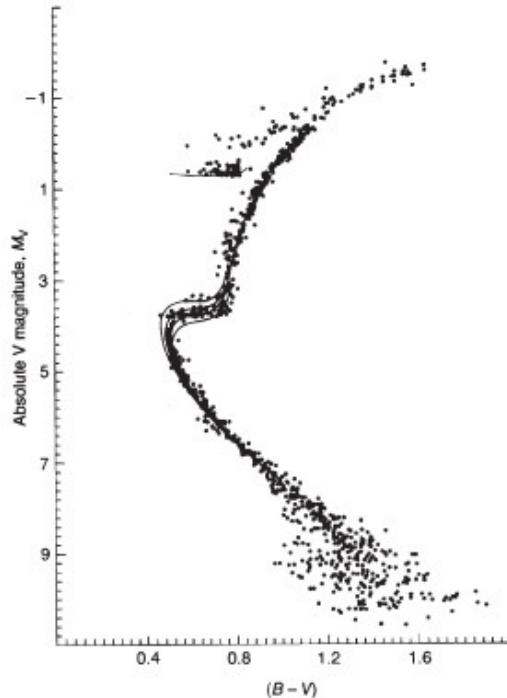
Bolte (1997) :
$$T_0 = 15 \pm 2.4 \, (\text{stat})^{+4}_{-1} \, (\text{syst}) \, \text{Gy}$$
Chaboyer (1998) :
$$T_0 = (11.5 \pm 1.3) \, \text{Gy}$$

Nucleocosmochronology

CS 22892-052 has iron abundance is 1000 times less than the solar value. A number of species never previously observed in such metal-poor stars were detected, as well a single line of thorium. A lower limit to the age of the star is

$$(15.2 \pm 3.7) \times 10^9 \text{ years}.$$

Schramm found a lower limit to the age of the Galaxy of 9.6×10^9 years and his best estimates of the age of the Galaxy are somewhat model-dependent, but typically ages of about $(12 - 14) \times 10^9$ years.

Gravitational Lensing and Dark Matter
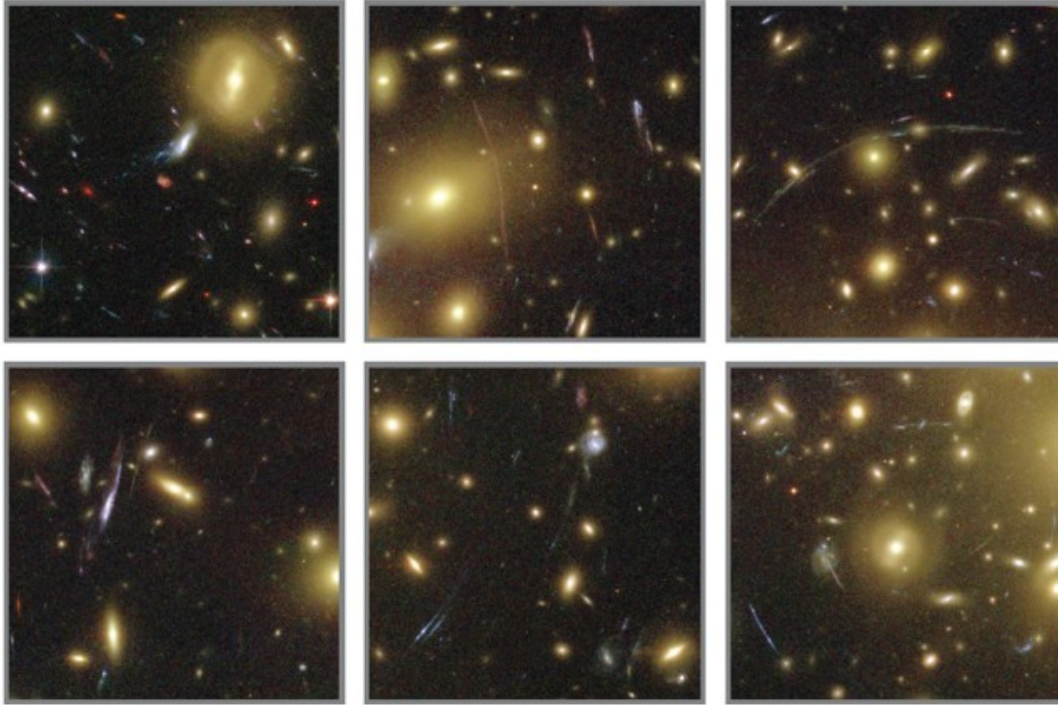
Detailed images of the galaxy cluster Abell 1689 showing numerous arcs that are images of lensed background galaxies distorted by the gravitational field of this massive cluster.

Weak gravitational lensing provides direct evidence about the distribution of dark matter in galaxies, clusters and large scale structures.

Statistics of Gravitational Lenses

Are the numbers of gravitationally distorted images consistent with the standard model?

Statistics of Gravitational Lenses

In the Cosmic Lens All Sky Survey (CLASS): a very large sample of flat spectrum radio sources were imaged by the Very Large Array, Very Long Baseline Array and the MERLIN long-baseline interferometer.   13 sources were multiply imaged out of a total sample of 8958 radio sources . In 2005 they report a point-source lensing rate to be one per 690 ± 190 targets. The numbers are consistent with flat world models with density parameter

$$\Omega_0 = 0.31 \pm 0.25 \pm 0.12 \text{ (systematic)}.$$

For a flat universe with dark energy equation of state of the form $p = w\rho c^2$, they found an upper limit $w < -0.55 \pm 0.15$ consistent with $w = -1$.

The Density Fluctuation Spectrum including Other Data
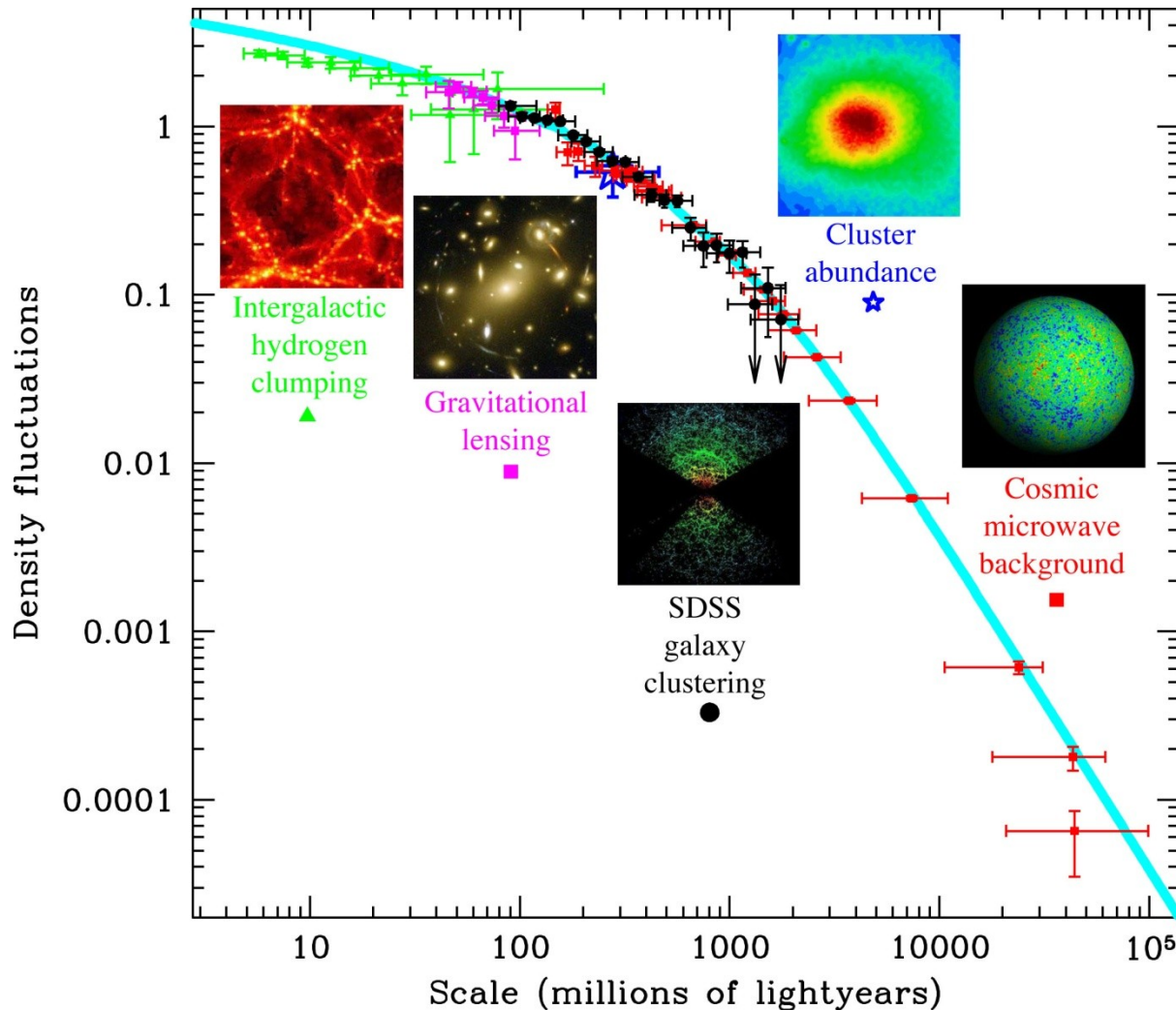
Blue line is the standard Harrison-Zeldovich spectrum with *n = 1*.

The Properties of the Concordance Model

The scale factor-cosmic time relation for $\Omega_0 + \Omega_\Lambda = 1$ model is

$$t = \int_{t_1}^{t_0} dt = -\frac{1}{H_0} \int_{\infty}^{z} \frac{dz}{(1+z)[\Omega_0(1+z)^3 + \Omega_\Lambda]^{1/2}},$$

where $a = (1+z)^{-1}$. This results in an accelerating Universe at the present epoch.

If $\Omega_\Lambda = 0.72$ and $\Omega_0 = 0.28$, the age of the world model is

$$T_0 = 0.983 H_0^{-1} = 1.32 \times 10^{10} \text{ years.} \tag{21}$$

Thus, $T_0 \equiv H_0^{-1}$. Is this a coincidence? In the standard ΛCDM model, the answer is "Yes".
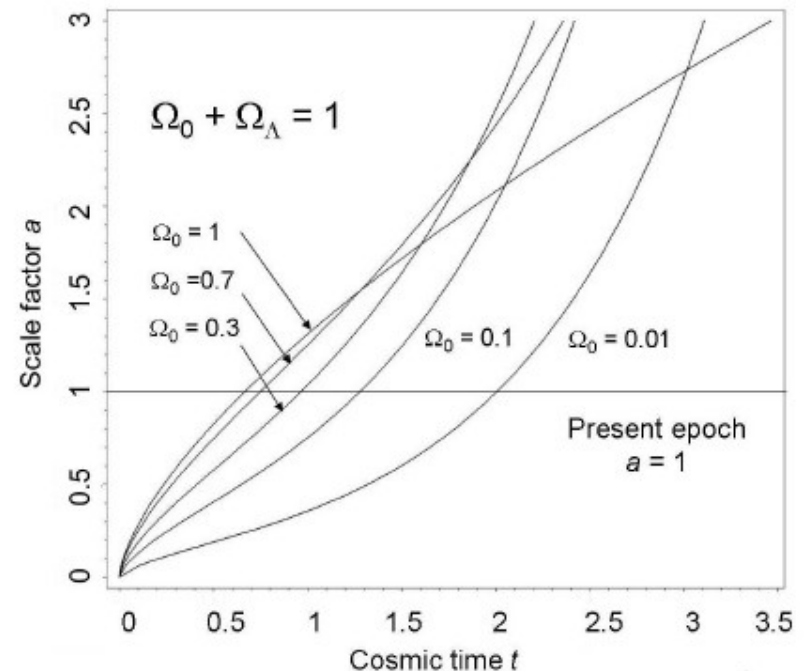
The Basic Problems

- Why is the Cosmic Microwave Background Radiation so isotropic?

- Why is the Universe geometrically flat, $\Omega_K \approx 0$?

- Why is the Universe baryon-asymmetric with

$$N\gamma/N_B = 1.6 \times 10^9.$$

- Why do the cosmological parameters take the values $\Omega_\Lambda \approx 0.72$, $\Omega_D \approx 0.23$, $\Omega_B \approx 0.05$ and Ω_Λ is 10^{120} too small?

- What is the origin of the initial power spectrum of perturbations and why is it close to power-law form?

Solutions

- That is just how the Universe is – the initial conditions were set up that way.

- There are only certain classes of Universe in which intelligent life could have evolved. This approach involves the *Anthropic Cosmological Principle* according to which the Universe is as it is because we are here to observe it.

- The inflationary scenario for the early Universe.

- Seek clues from particle physics and extrapolate to the earliest phases of the Universe.

- Something else we have not yet thought of. This would certainly involve new physical concepts.

The Inflationary Solution
Inflation without Physics

Standard Big Bang

10^{19} GeV

Temperature T

Scale factor

10^{14} GeV

Factor of 10^{31} in R

3 K

10^{-43} s 10^{-34} s   Today
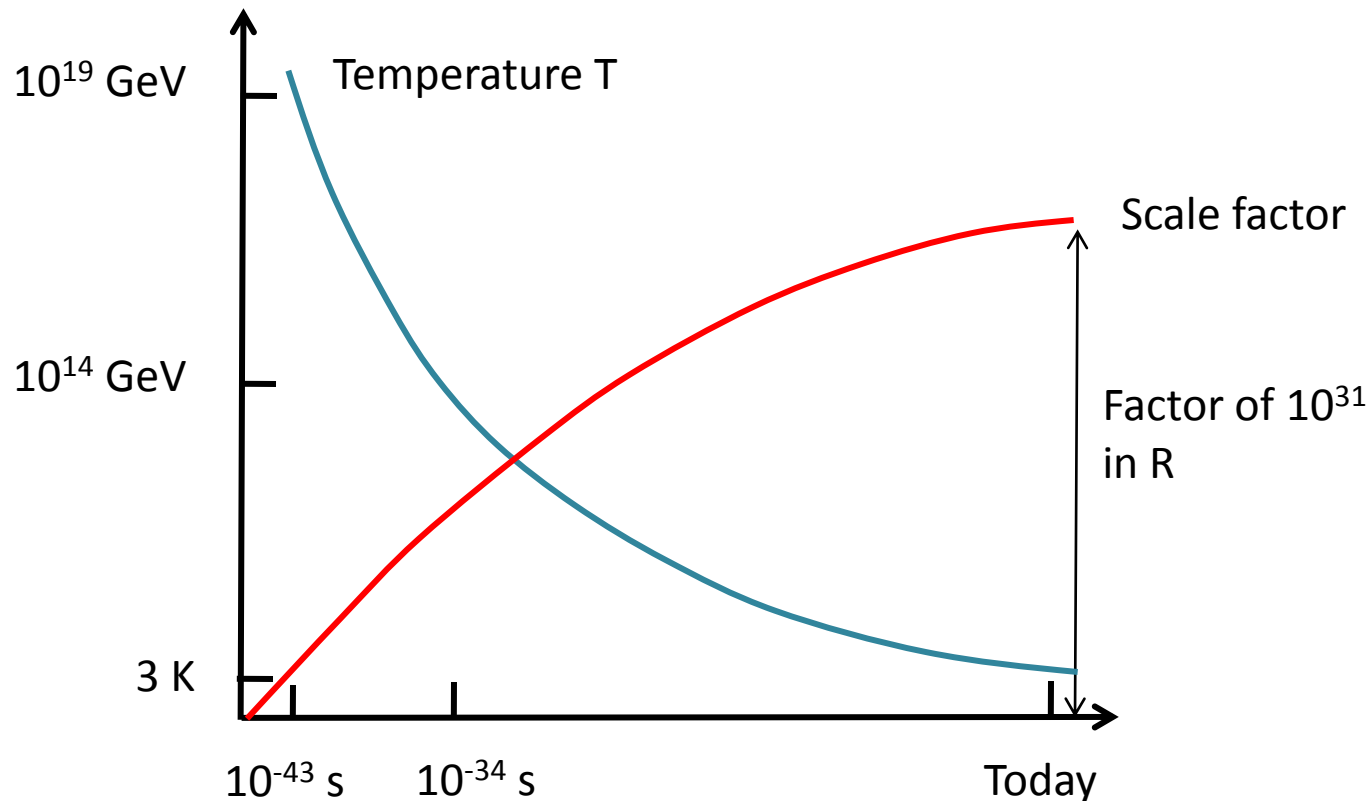
The Inflationary Solution
Inflation without Physics

Standard Big Bang with Inflation
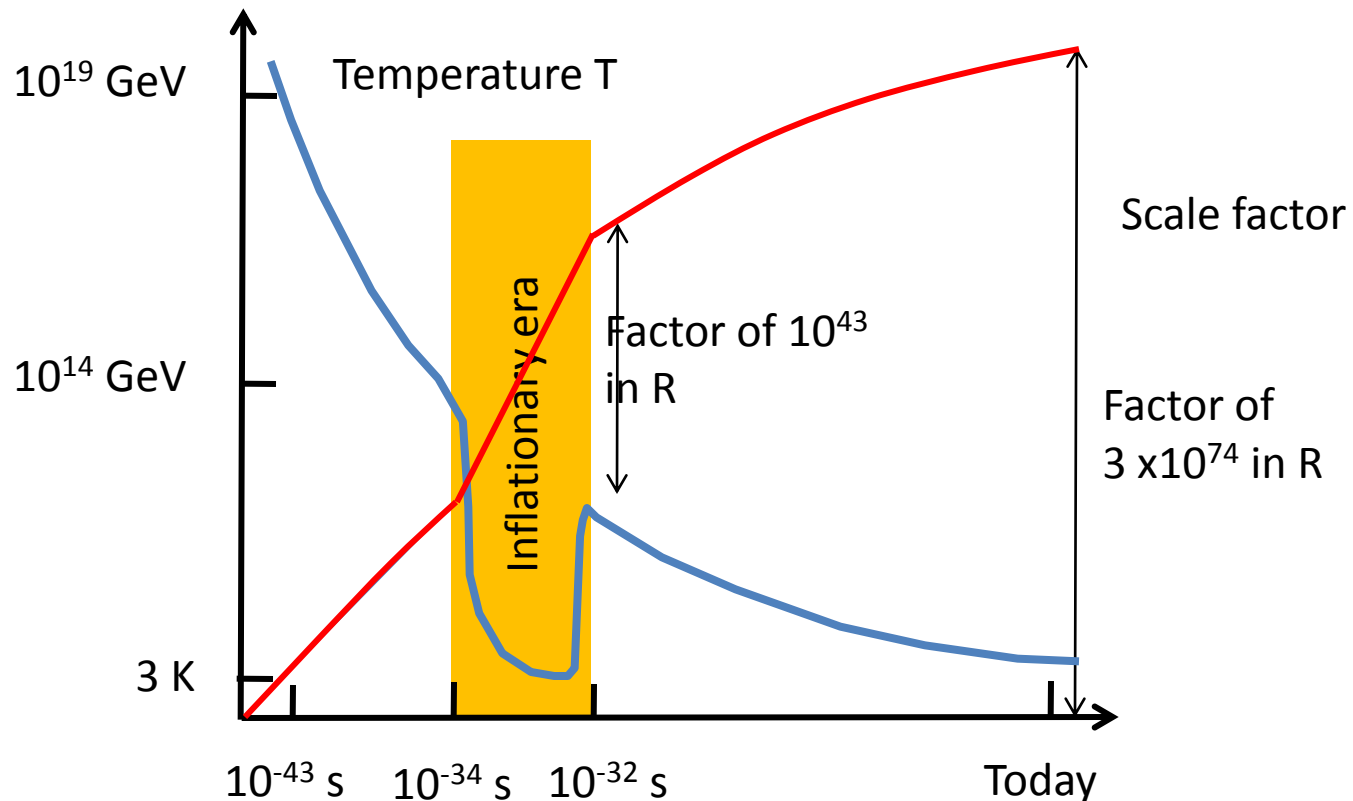
Inflation without Physics

- The effect of the early inflationary phase is to drive particles outside their local particle horizons. If there were sufficient e-folding times, particles which were originally in causal contact in the very early Universe and so could homogenise the material of the Universe, were driven far beyond their causal horizons by the present epoch, solving the horizon problem.

- The inflationary expansion also straightens out the geometry of the Universe, however complex it may have been in the early Universe. The Universe is driven to flat geometry at the present epoch.

Inflation with Physics

- To convert this idea into a physical theory, we need to appeal to scalar fields which have exactly the right properties to derive an exponential expansion. Their equation of state can be written

$$\varrho_\phi = \frac{1}{2}\dot{\phi}^2 + V(\phi)$$

$$p_\phi = \frac{1}{2}\dot{\phi}^2 - V(\phi)\,.$$

- If the first terms, the kinetic energy terms, are very small compared with the potential energy terms, we obtain a negative pressure equation of state $p = -\rho c^2$.

Inflation with Physics – the Good News

- The Inflationary picture has, however, a remarkable property which was not expected when it was first proposed. We need to consider the quantum fluctuations in the scalar fields during the inflationary era during the very early Universe

- Amazingly, in the simplest model of inflation, the fluctuations in the scalar field result in exactly the Harrison-Zeldovich spectrum, $P(k) \propto k$.

Future Challenges

- The PLANCK mission of ESA and an order of magnitude improvement in the determination of cosmological parameters

- Is the physics of the standard model accurate at the 1% level?

- The evolution of galaxies and large scale structures – do they really agree with the prediction of the standard ΛCDM model?

- Is the dark energy really the cosmological constant (EUCLID) – what is the value of w?

- Does the dark energy vary with cosmic epoch (EUCLID)?

- Clues from the LHC at CERN – Higgs particles + dark matter particles?

- Direct detection of dark matter particles

- There are many large scale surveys planned to address these issues.

Testing General Relativity

- Testing all aspects of general relativity in the laboratory and in space.

- The availability of clocks with precision one part in 10^{18}.

- At this level, there may well be detectable effects of extra dimensions and other modifications to General Relativity.

- In principle, we can get to one part in 10^{21}.

- Tests of gravity in the strong field limit.

Euclid project of ESA
(see also recommendations of the US Decadal Review)
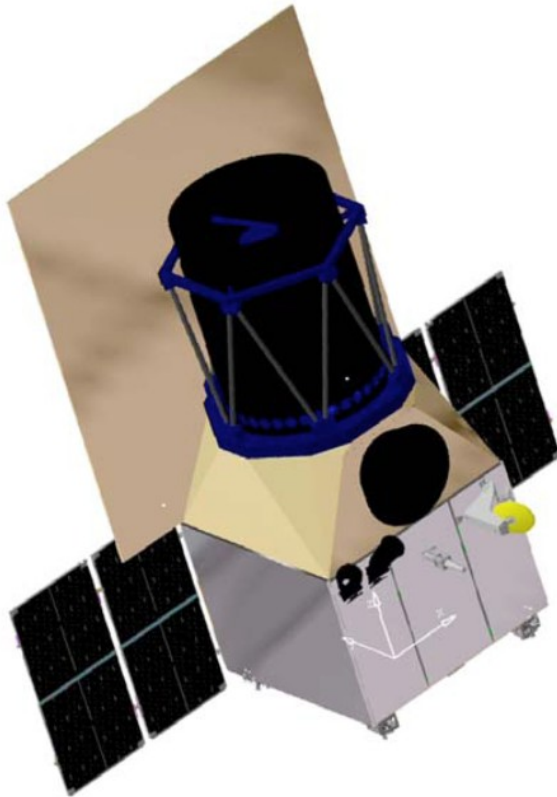
- Baryon Acoustic Oscillations (BAO), Weak Gravitational Lensing (WL), deviations from GR

- Huge samples of galaxies with colours/spectra

Overview – The Euclid Concept

High precision and accurate DE measurements require a combination of two or more probes. Euclid aims at the most promising dark energy probes: an all sky survey of weak lensing (WL) and galaxy redshifts for baryon acoustic oscillations (BAO).

- Individually, the two are the most powerful measures of dark energy.

- In combination they will control and measure a wide range of systematics. Cross correlation between galaxy positions and shear will measure number counts versus density.

- Enables breaking degeneracies in parameter space

- The combination measures the two Newtonian potentials $\phi(k,z)$ and $\psi(k,z)$, which describe a perturbed LFRW Universe.

Testing General Relativity on Large Scales

The general first-order perturbation of the Robertson-Walker metric allows models differing from General Relativity through the separate measurement of the perturbation potentials $\phi(k,z)$ and $\psi(k,z)$. Their ratio is equivalent to the quantity γ which appears in the PPN formalism of general metric theories of gravity. In the conformal Newtonian gauge

$$ds^2 = a^2(\tau)[(1+2\phi)d\tau^2 - (1-2\phi)(dx^2 + dy^2 + dz^2)]$$

The WL and BAO measurements depend in different ways upon $\phi(k,z)$ and $\psi(k,z)$ – WL on both ϕ and ψ, BAO on ψ - and so enable us to test if GR is the best description of gravity on the scale of the largest perturbations.

This contrasts with Solar System GR tests which test the linearity of gravity on a very small scale.

How is it done?

There are two independent ways in which precise estimates of the basic cosmological parameters can be estimated. Hubble's constant varies with scale factor a as:

$$H^2(a) = H_0^2 \left[\Omega_{\mathrm{m}} a^{-3} + \Omega_{\mathrm{rad}} a^{-4} + \Omega_{\mathrm{v}}(a) + \Omega_{\mathrm{k}} a^{-2} \right] .$$

If we write the vacuum equation of state $p = w\varrho c^2$ and w is a constant, we find $\Omega_{\mathrm{v}}(a) = \Omega_{\mathrm{v0}} a^{-3(w+1)}$. Thus, we only recover the standard cosmological constant if $w = -1$. We know that w is close to this value.

If the dark energy term varies with cosmic epoch, we need to replace the dark energy term by

$$\Omega_{\mathrm{v}}(a) = \Omega_{\mathrm{v0}} \exp \left(\int -3[w(a) + 1] \, \mathrm{d} \ln a \right) .$$

These changes are reflected in variations with redshift of the comoving radial distance coordinate, which appears in the relation between intrinsic properties to observables:

$$r(z) = \int_0^z \frac{c}{H(z')} \, \mathrm{d}z' .$$

How is it done?

The second method uses the growth of large scale structures as a function of cosmic epoch. The density contrast $\Delta = \delta \varrho / \varrho$, evolves with cosmic epoch as:

$$\ddot{\Delta} + 2\left(\frac{\dot{a}}{a}\right)\dot{\Delta} = \Delta\left(4\pi G\varrho_\mathrm{m} - \frac{c_\mathrm{s}^2 k^2}{a^2}\right) .$$
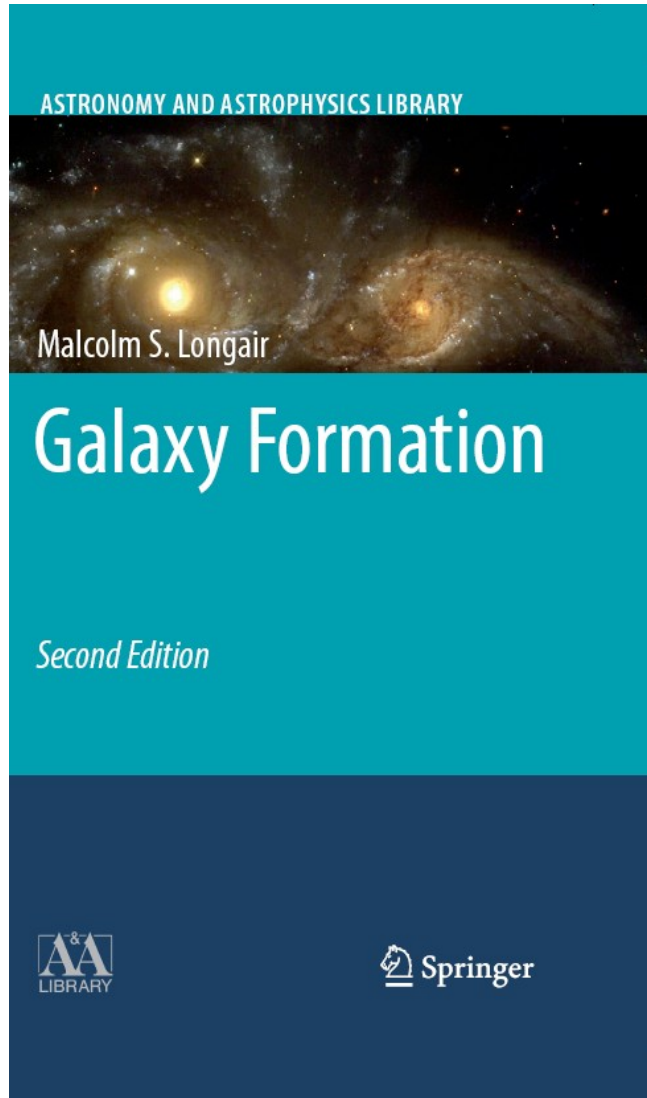
The sound speed c_s is zero for cold dark matter and the 'thermal' sound speed for baryon acoustic oscillations.

Thus, by measuring very precisely the comoving radial distance coordinate and the development of large scale structures in the cold dark matter and the baryons as functions of redshift, we test simultaneously the values of the cosmological parameters and their variation with cosmic epoch. The procedure also tests the validity of the general relativity on the very largest scales on which density perturbations are observed. The role of General Relativity appears on both sides of the equation, explicitly on the right, through the presence of G and implicitly through the dependence of $a(t)$.

Why is the combined Euclid mission so powerful?

- The weak lensing will reconstruct directly the distribution of the dark matter and the evolution of the growth rate of dark matter perturbations with redshift.

- The baryon acoustic oscillations act as standard rods, determine $P(k)$ and provide a measure of $H(z)$ and hence $w(z)$. They also map out the evolution of the baryonic component of the Universe.

- Together, these enable many systematic effects to be controlled – for example, intrinsic alignments in weak lensing, bias factors in baryon acoustic oscillations. Value of w to 1% - variation of $w(z)$ with redshift to 10%.

- Both act as independent dark energy probes. If they differ, we learn about modifications to GR.

For Many More Details

ASTRONOMY AND ASTROPHYSICS LIBRARY

Malcolm S. Longair

Galaxy Formation

Second Edition

A&A LIBRARY

Springer

The new edition was published by Springer Verlag in 2008. Many more details of the observations and calculations can be found there.

The emphasis is upon the basic physics involved in astro-physical and theoretical cosmology, keeping it as simple, but rigorous, as possible.

How it came about
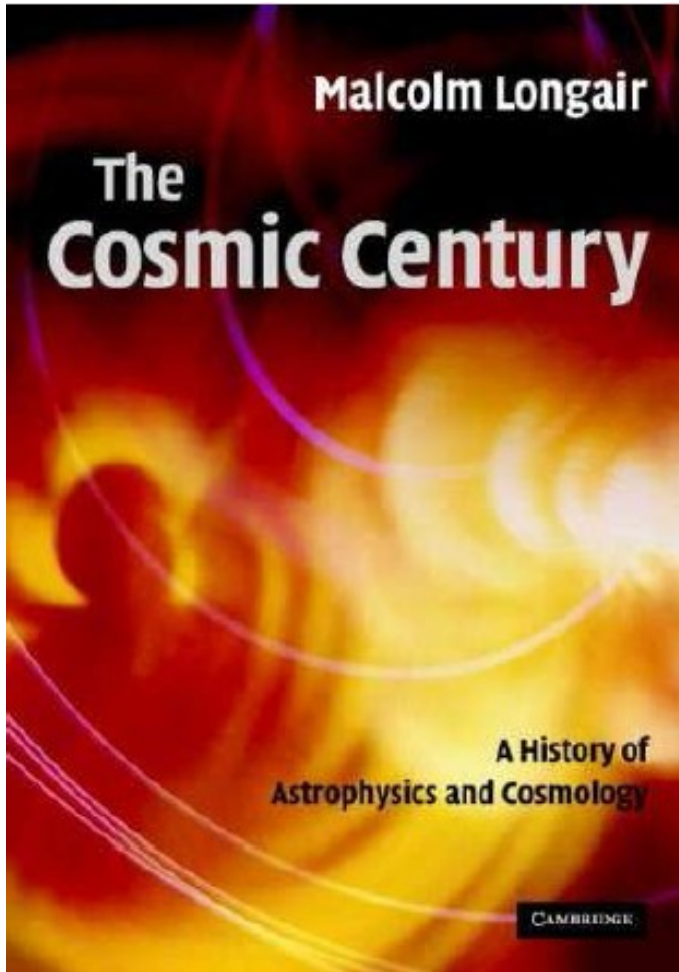
If you are interested in understanding the history of the development of cosmology, you may find my book The Cosmic Century (2006) useful. It covers the history of cosmology up to 2005.